

Biomedical Optical Imaging¹

Tutorial Presented at:
2007 IEEE International Symposium on Biomedical Imaging
April 12, 2007
Washington, D.C.

Charles A. Bouman
School of Electrical and Computer Engineering
School of Biomedical Engineering
Purdue University
(765) 494-0340
bouman@purdue.edu
www.ece.purdue.edu/~bouman

With contributions from:
Guangzhi Cao, Vaibhav Gaind, Kevin Webb
School of Electrical and Computer Engineering
Purdue University
and
Adam Milstein, and Seungseok Oh

¹Special thanks to Dr. John Cozzens and the National Science Foundation for supporting this work under contracts CCR-0073357 and CCR-0431024.

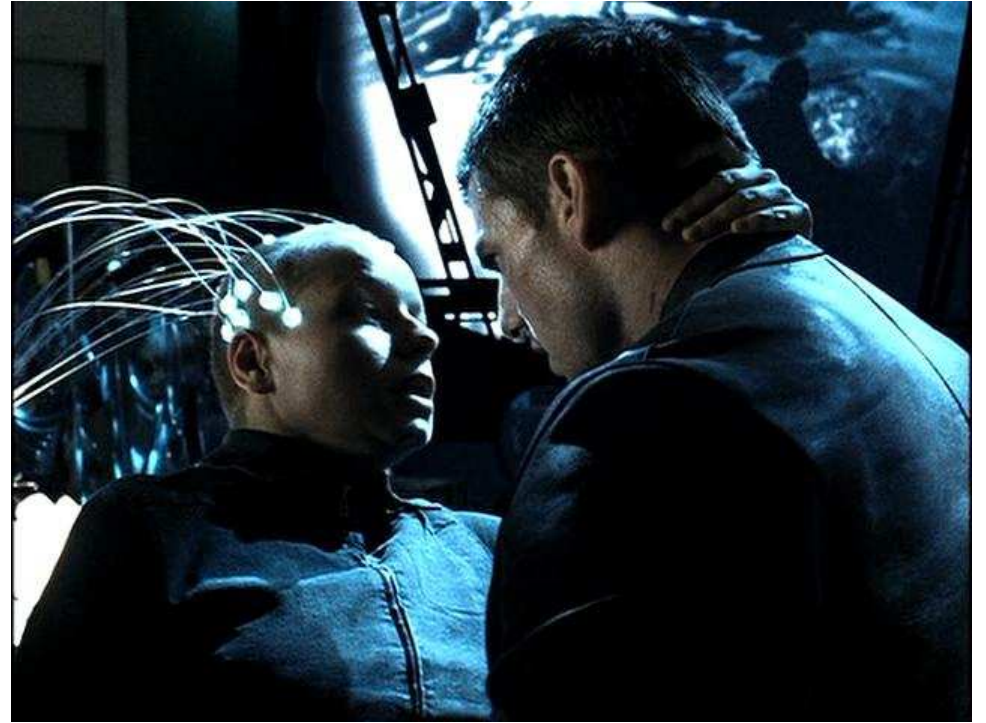
Part I: Introduction to Biomedical Optical Imaging and Applications

1. Interactions of tissue and light
 - (a) Propagation of light in tissue
 - (b) Light sources, lasers and non-coherent sources
 - (c) Fluorescence, fluorephores, ICG, and GFP
 - (d) Bioluminences and luciferase
 - (e) Raman spectroscopy
2. Applications of bio-optical imaging
 - (a) Optical contrast agents
 - i. Folate-Targeted fluorescence
 - ii. Quantum dots
 - (b) Molecular Imaging
 - i. What is molecular imaging?
 - ii. How can it be used?
 - (c) Microscopic imaging modalities
 - i. Fluorescence microscopy
 - ii. Confocal microscopy
 - iii. Multiphoton microscopy
 - iv. Nonlinear microscopy techniques - PALM, FLIM
 - (d) Optical Coherence Tomography
 - (e) Optical Diffusion Tomography
 - i. ODT methods and Systems
 - ii. Fluorescence ODT
 - iii. Brain imaging
 - iv. Breast imaging
 - v. Small animal imaging

Seeing Inside the Body with Light?

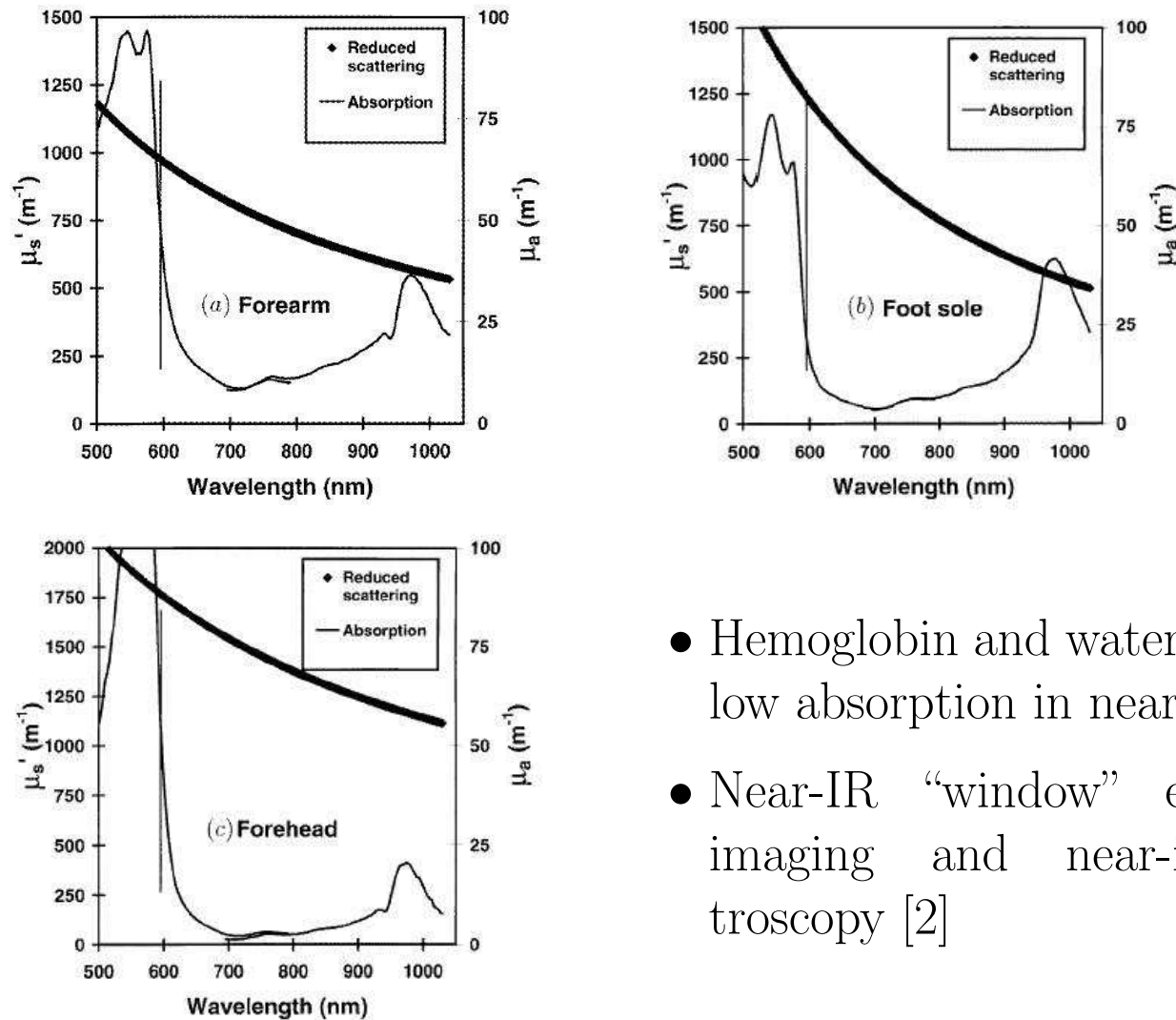


Minority Report, Twentieth Century Fox, 2002.



Wally: “We scan, by way of *optical tomography*, white light pinpoints pulse along the entire length of the headgear, and re-read after absorption through their brain tissue.”

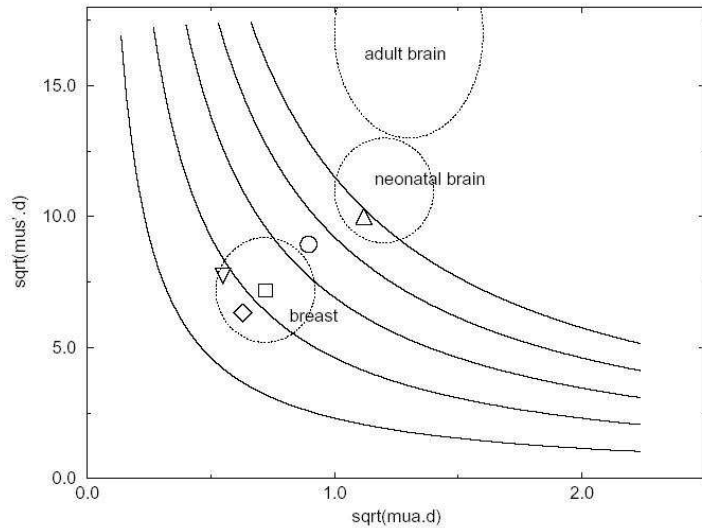
Transparency of Tissue in Near-IR Range [1]



- Hemoglobin and water have relatively low absorption in near-IR
- Near-IR “window” enables optical imaging and near-infrared spectroscopy [2]

(Reproduced from [1] R. M. P. Doornbos *et al.*, *Phys. Med. Biol.*, 1999.)

Near-IR Window [3]

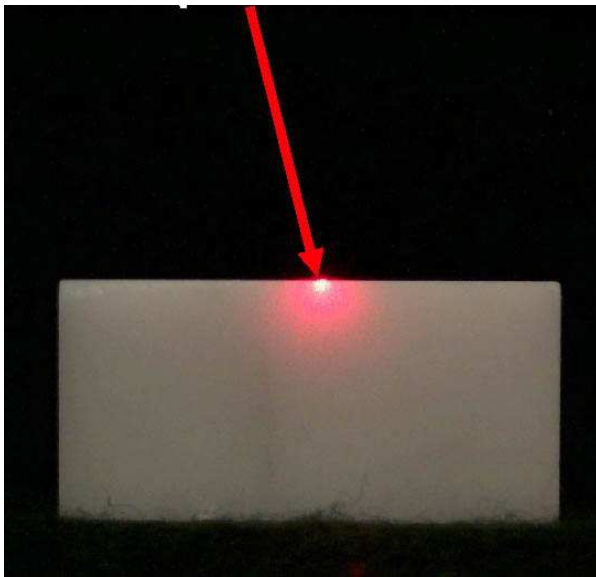


- Abscissa and ordinate axes are $(\mu_a d)^{1/2}$ and $(\mu'_s d)^{1/2}$, respectively, where d is the size of the reconstruction object
- Curved lines are constant $(\mu_a \mu'_s)^{1/2} d$ and represent approximately equal attenuation, at intervals of powers of 10
- Dotted circles represent approximate values for tissues of interest
- The range of optical coefficients vary by orders of magnitude for different tissues

(Reproduced from [3] S. R. Arridge, *Inverse Problems*, 1999.)

Light Source

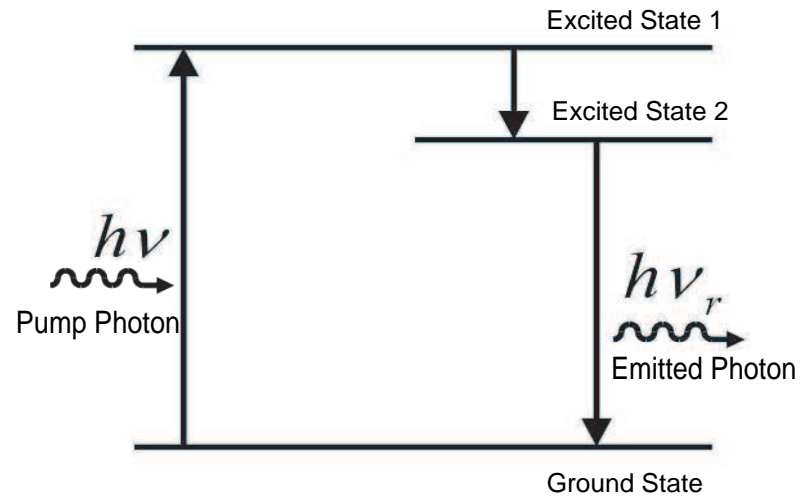
- Coherent laser source
 - Parameters: power, wavelength
 - Tunable: Ti-Sapphire lasers
 - Not tunable: Diode lasers, solid-state laser
 - Application: 2-photon microscopy
- Non-Coherent light sources
 - Examples: white light sources, xenon arc lamp.
 - Application: confocal microscopy



Diffusion of laser light in a marble sample [4]

(Reproduced from [4] G. Godin, 2001)

Fluorescence



- Fluorescence results from radiative decay from an excited state
- Basic concept from two-level rate equation analysis [5]

Fluorescence: Two-Level Rate Equation[5]

- Notation:

N_1 and N_2 - number of electrons in ground and excited states

$\Delta N(t) = N_1(t) - N_2(t)$ - number of electrons in an excited state

$W_{12} = W_{21}$ - rate of upward or downward transition

- Fixed total population \rightarrow one rate equation
- Optical frequency transition \rightarrow spontaneous emission rates dominate thermally stimulated rates

$$\frac{d}{dt}\Delta N(t) = -2W_{12}\Delta N(t) - \left[\frac{\Delta N(t) - \Delta N_0}{\tau_{21}} \right]$$

- $-\left[\frac{\Delta N(t) - \Delta N_0}{\tau_{21}} \right]$ causes population difference to relax to thermal equilibrium (ΔN_0) with time constant τ_{21}
- τ_{21} is the fluorescence lifetime of fluorephore
- W_{12} proportional to strength of applied signal

Fluorescent Marker 1: Fluorophore Indocyanine Green (ICG) [6]

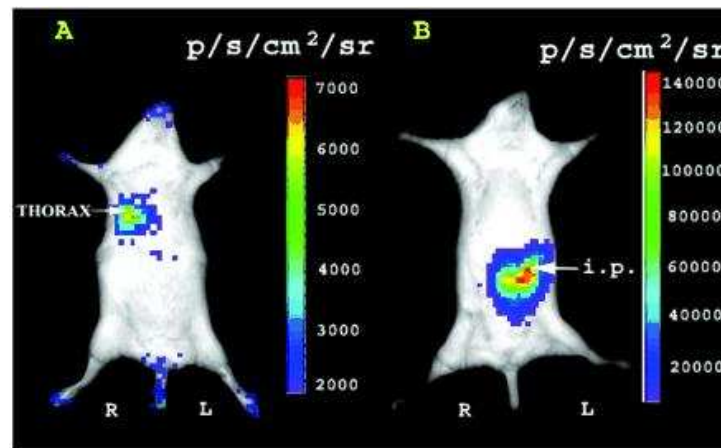
- A tricarbo-cyanine dye with infrared absorbing properties
- Pumped at 780 nm and emits at approximately 830 nm
- Important because of its peak absorption and emission is in IR range where tissue absorption is smallest
- Has little or no absorption in the visible range
- Can be used in humans [6]

Fluorescent Marker 2: Green Fluorescent Protein (GFP) [7]

- Protein that fluoresces green when exposed to blue light
- Pumped at 395 nm and emits at 509 nm
- Can use reporter gene to produce GFP in small sets of specific cells
- Less harmful to living cells than fluorescein isothiocyanate
- Transgenic mice with cells that express the GFP reporter gene are used for *in vivo* imaging of neurons

Bioluminescence Marker: Luciferase [8]

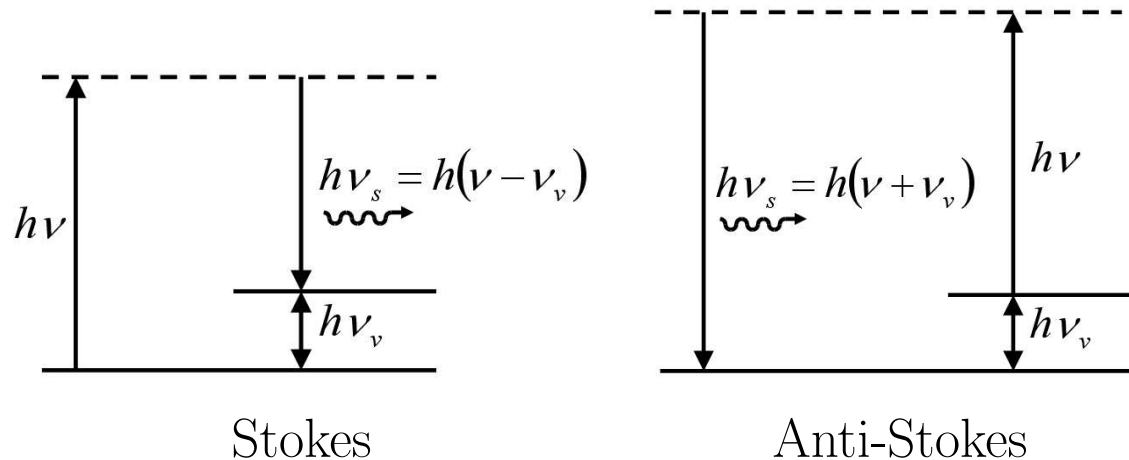
- Bioluminescence: enzymes catalyze a bio-chemical process inside the animal that emits light
- Luciferase: emits visible light when it combines with Luciferin + ATP + O_2
- Example: light from firefly
- Does not require any external excitation
- Can be used for molecular imaging



(Reproduced from [8] S. Bhaumik *et al.*, *PNAS*, 2002)

Raman Spectroscopy: Basics

- Raman scatter results from coupling to molecular vibrations [9]
- Each molecule has a unique Raman spectra (fingerprint spectra)
- Typical Raman cross-section, $\sigma \sim 10^{-29} \text{ cm}^2 \text{ molecule}^{-1} \text{ sr}^{-1}$. Very weak signal.

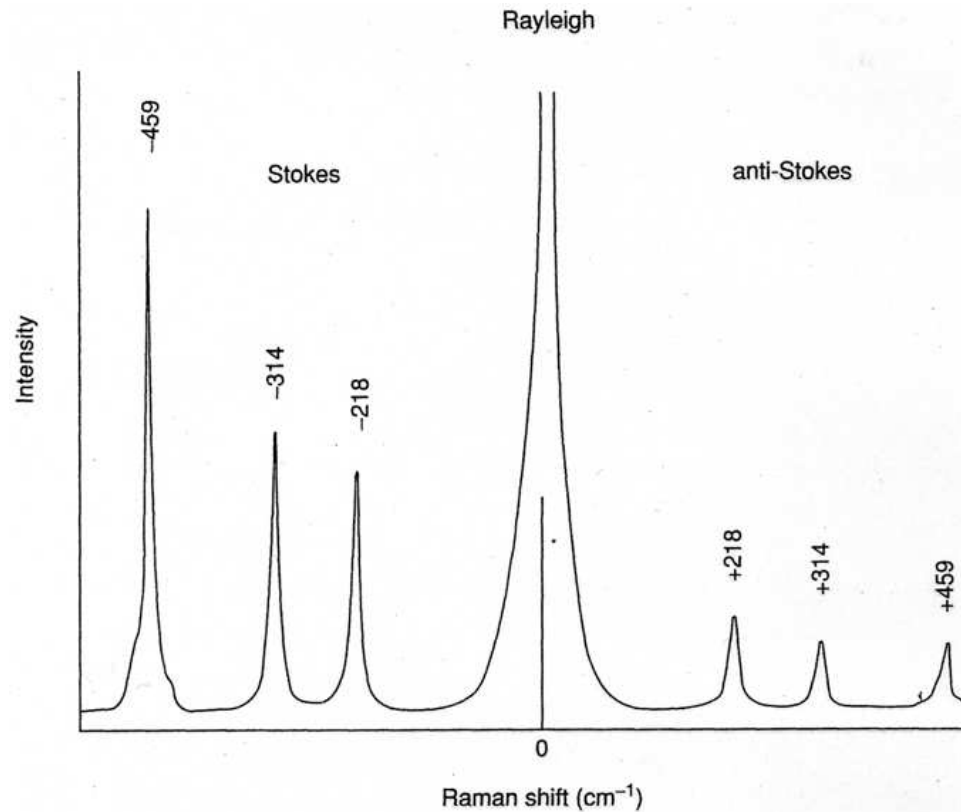


- Wave number: $\tilde{\nu} = \nu/c$
- $\lambda = 1 \text{ } \mu\text{m}$, $\Delta\tilde{\nu} = 100 \text{ cm}^{-1}$ [9] $\rightarrow \Delta\lambda = 10 \text{ nm}$, $\Delta\nu = 3 \text{ THz}$

C. V. Raman and K. S. Krishnan, *Nature*, **121**, 501 (1928)

Raman Spectroscopy: Example

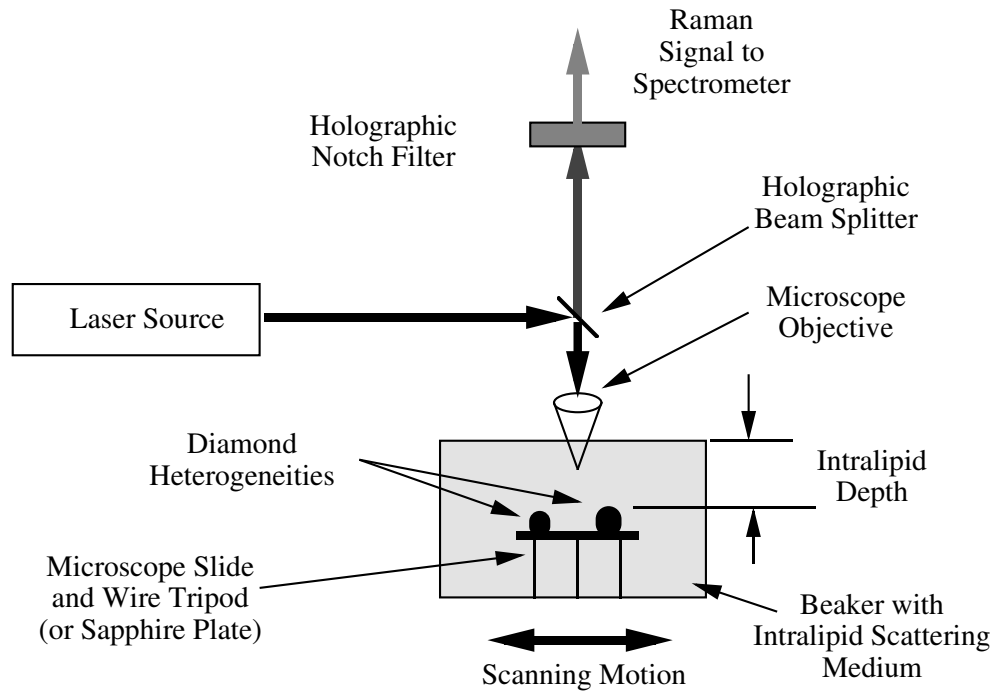
- Example Raman spectrum for CCl_4 with 488 nm excitation[10]



J. R. Ferraro, K. Nakamoto and C. W. Brown, *Introduction to Raman Spectroscopy*, Academic Press, 2003.

Raman Spectroscopy: Imaging

- Scan detector and measure counts in a specific Raman line [11]

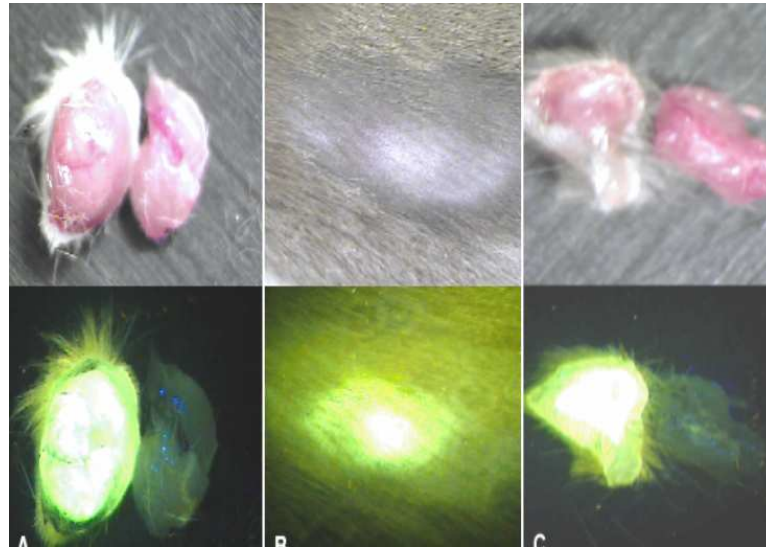


- Glucose? [12]

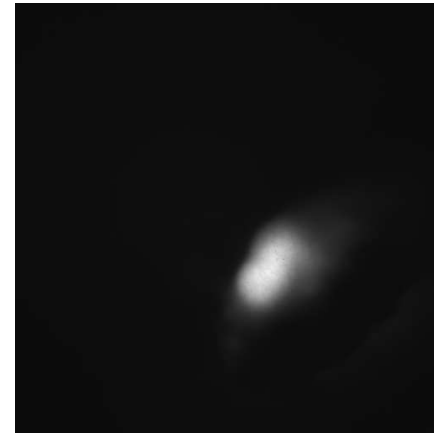
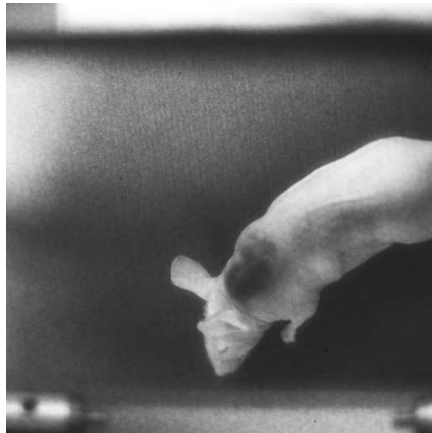
Targeted Contrast Agents

- Clinical diagnostic imaging often relies on different uptake behavior between tumors and the surrounding tissue
- Non-targeted dyes may accumulate in tumor due to increased vascular density or capillary permeability [13]
- Some imaging agents specifically target certain receptors which are overexpressed in malignant cells
- Examples of targeting ligands for delivery of diagnostic imaging agents include antibodies[14], hormones [15], small peptides [16], and folic acid [17]

Folate-Targeted Fluorescent Agents[17, 18]

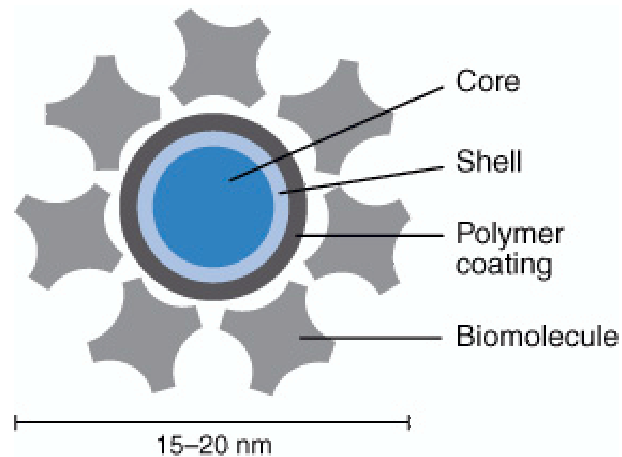


Mouse tumors containing folate-fluorescein

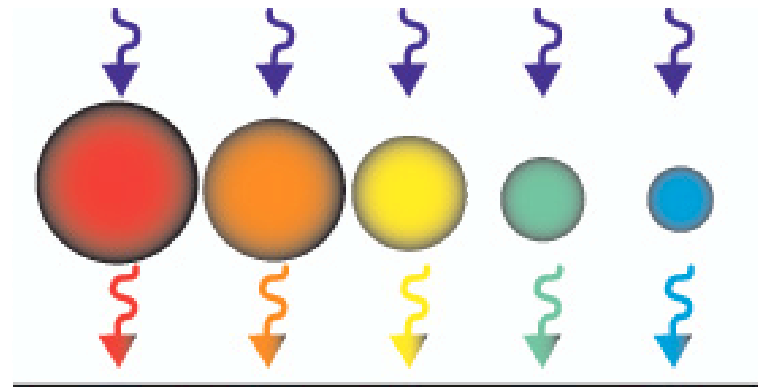


Mouse tumors containing folate-indocyanine

Quantum Dots for Imaging Living Cells [19]



Quantum dot structure

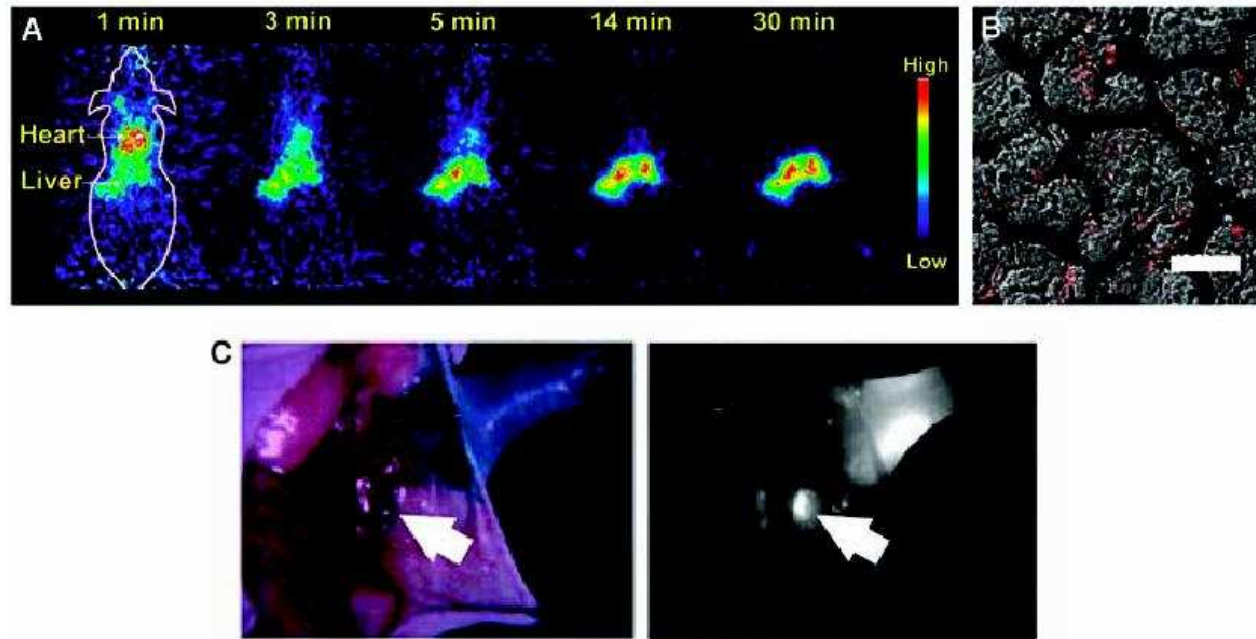


Tuneability of quantum dot

- High quantum yield (90%)
- Tunable emission wavelength by changing the Qdot size
- Resistance to bleaching- useful for 3-D imaging.
- Broadband absorption spectrum compared to standard fluorphores

(Reproduced from <http://probes.invitrogen.com/products/qdot/overview.html>)

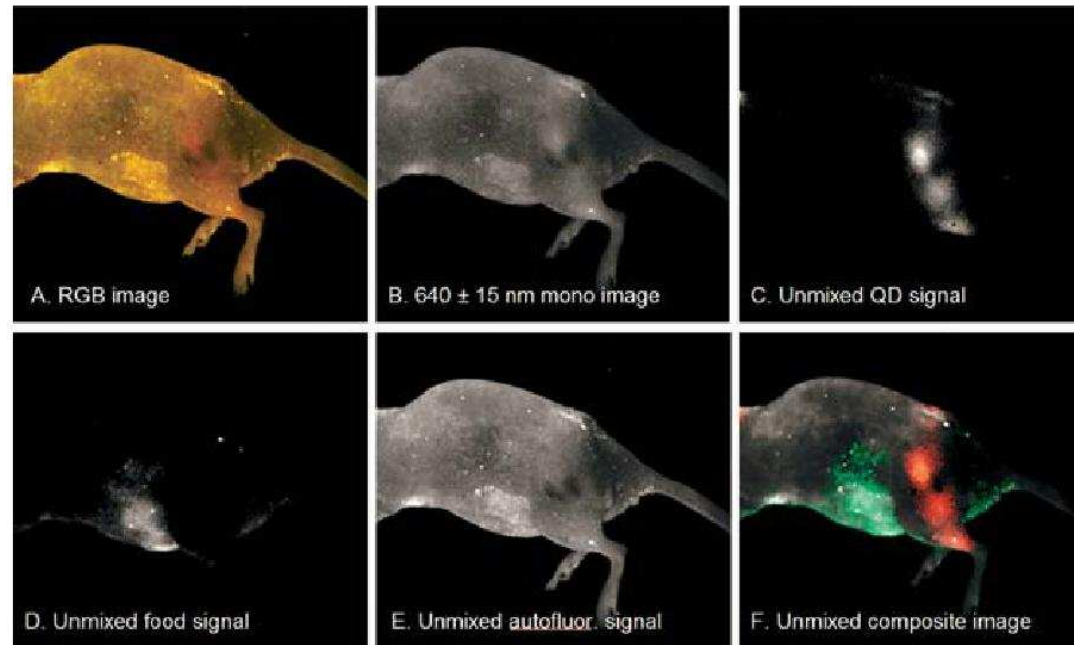
Quantum Dots for Imaging Living Cells [19]



- Long fluorescence lifetime enables removal of cell autofluorescence
- Toxicity: can not be used in humans

(Reproduced from [19] X. Michalet *et al.*, *Science*, 2005)

Quantum Dots for Multispectral Imaging [20]



- Emission wavelength tuneability enables multispectral imaging and spectral multiplexing
- Deep-tissue imaging

(Reproduced from [20] J. Mansfield *et al.*, *J. Biomedical Optics*, 2005)

Molecular Imaging: What is it?

- Create methods to image the underlying biological processes or functional state of living cells, tissues, and organs.
- In vivo imaging of living organisms
- Can use MRI, PET, SPECT, or optical imaging modalities
- Applications:
 - Detect disease in humans
 - Quantify disease in small animals for drug development
 - Better understand biological processes in living animals

Molecular Imaging: Some Definitions

- **Gene expression:** Not all genes are active once cells differentiate. When a gene is being expressed, it produces its associated protein. It is often important to know when a gene is being expressed.
- **Reporter genes:** Reporter genes can be “attached” to genes of interest. When the gene of interest expresses itself, the reporter gene also expresses itself. Typically, the reporter gene produces a protein which can be easily detected using an imaging modality.
- **Gene therapy:** A set of methods for changing the genes in the cells of living animals by adding DNA to the cells. One common way of doing this is to use a modified virus as a “vector” to deliver the DNA gene sequence to the living cells.
- **Transgenic animals:** Animals that have had their genes artificially modified are known as transgenic animals. This might be done using gene therapy or by changing the genetic structure of an animal embryo before implanting it in the uterus of a surrogate mother.

Molecular Imaging: Imaging Gene Expression

Step 1: Select an animal model of interest

- For example a mouse “model” is commonly used

Step 2: Select a gene of interest

- You may want to know when and where this gene is being expressed in the mouse

Step 3: Select a reporter gene

- GFP - will fluoresce when excited by light
- Luciferase - lights up when it combines with Luciferin + ATP + O_2
- Luciferin is typically given to mouse intravenously when the imaging is performed.

Step 4: Image the mouse

Molecular Imaging: Drug Testing

Step 1: Select an animal model of interest

- For example a mouse “model” is commonly used

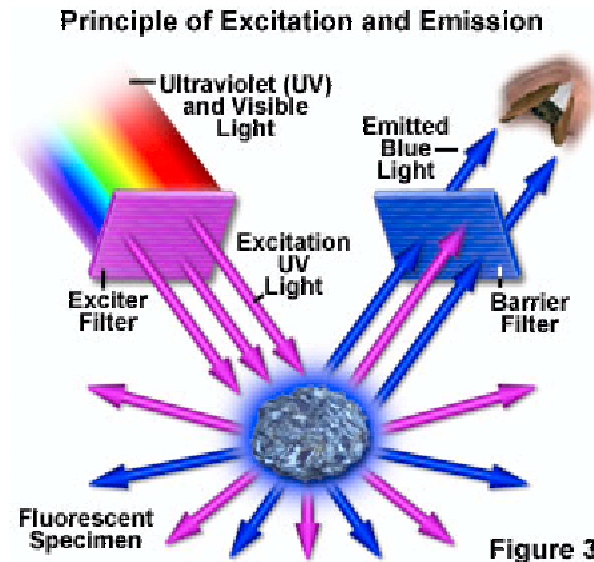
Step 2: Inject a small amount of transgenic tumor tissue

- Tumor contains gene for GFP or Luciferase

Step 3: Apply experimental drug

Step 4: Quantify tumor size with optical imaging method

Fluorescence Microscopy



- Based on the principle of absorption and re-radiation of light by fluorophores (like the Green Fluorescence Protein) in a specimen
- Provides higher contrast than conventional optical microscopies
- Resolution is diffraction limited
- Image is further blurred due to fluorescence from out-of-focus region of the specimen

(Reproduced from www.olympusmicro.com/primer/lightandcolor/fluorointroduction.html)

Confocal Microscopy

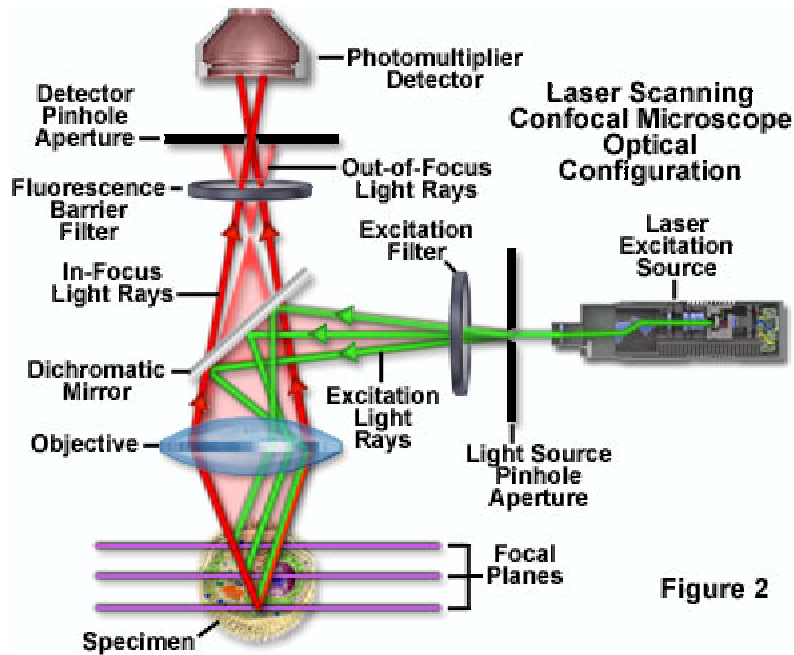
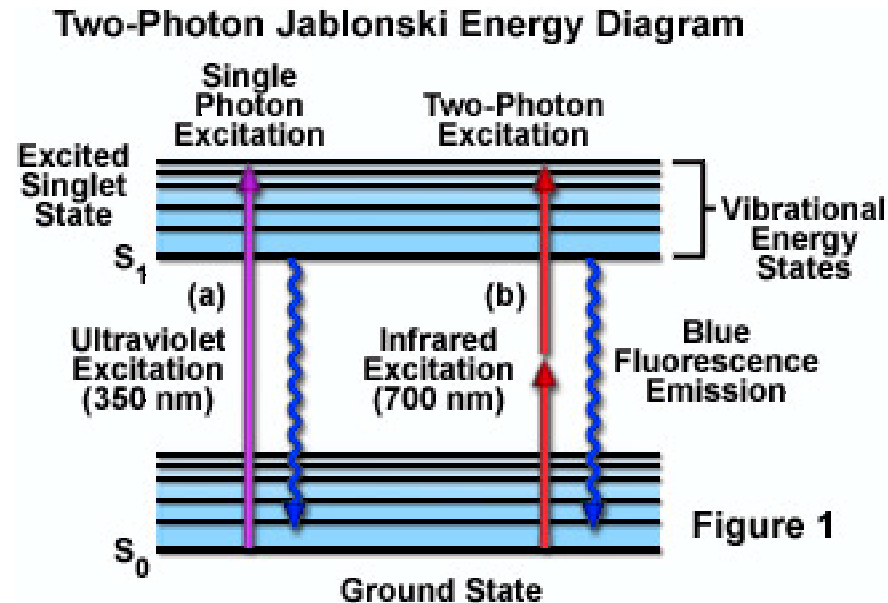


Figure 2

- In a confocal microscope, a focused beam is scanned across the specimen. Both the excitation and reemitted light are focused through lens.
 - The fluorescence emission that occurs above and below the focal plane is not confocal with the Pinhole aperture. Thus only the fluorescence emission from the laser focal point reaches the detector.
 - The confocal microscope facilitates the collection of three dimensional data
- Conventional fluorescence microscopes have poor resolution due to secondary fluorescence from out-of-focus regions.

(Reproduced from www.olympusfluoview.com/theory/confocalintro.html)

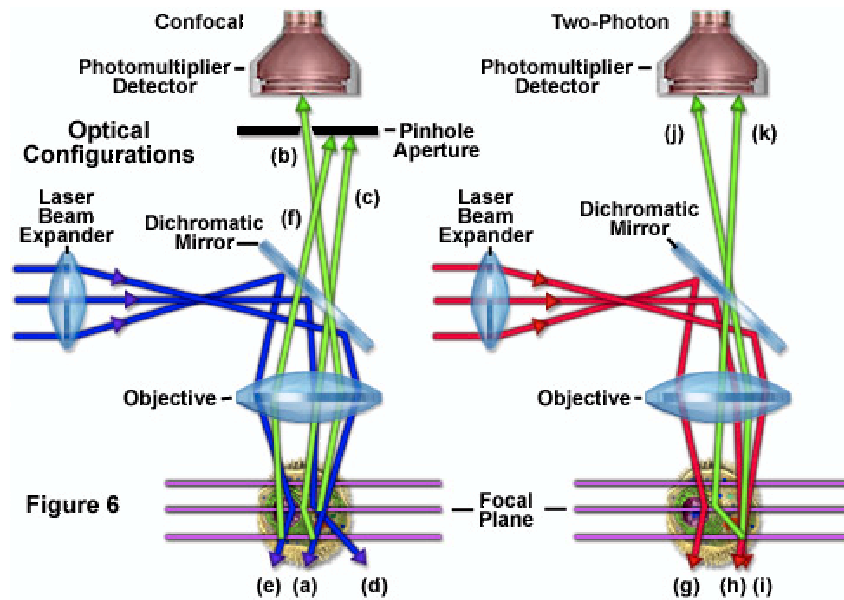
Two Photon Excited Fluorescence Emission



- Two low energy photon absorption
- Emission wavelength is shorter than excitation wavelength.
- Typical fluorophore emission wavelength is in the 400-500 nm range.
- Typical laser excitation wavelength is in the 700-1000 nm range.

(Reproduced from www.microscopyu.com/articles/fluorescence/multiphoton/multiphotonintro.html)

Two Photon Excited Fluorescence (TPEF) Microscopy



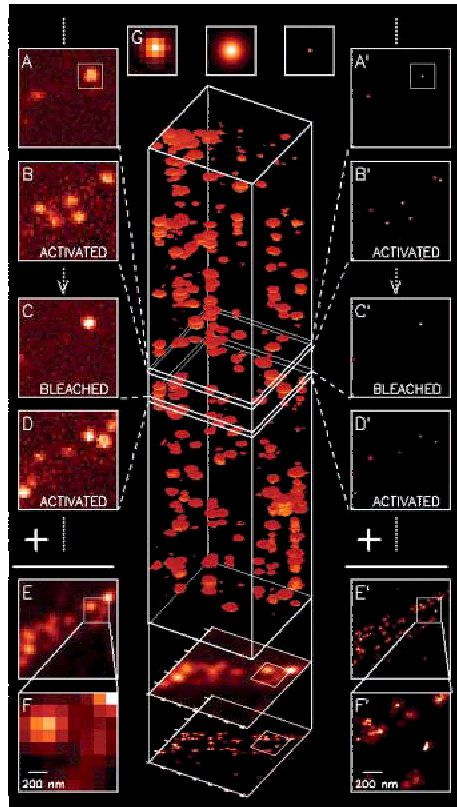
- Two photon absorption is a low probability event. Fluorescence emission emanates from the laser focus where photon density is greatest.
- Almost all emitted light comes from focal spot of laser.
- Less scattering and absorption of incident light in specimen due to NIR excitation.
- In a confocal setup, pinhole aperture rejects desired fluorescent photons scattered in the specimen. But in TPEF, all the light is collected.

Reproduced from:

www.microscopyu.com/articles/fluorescence/multiphoton/multiphotonintro.html

Photoactivated Localization Microscopy (PALM)

[21]

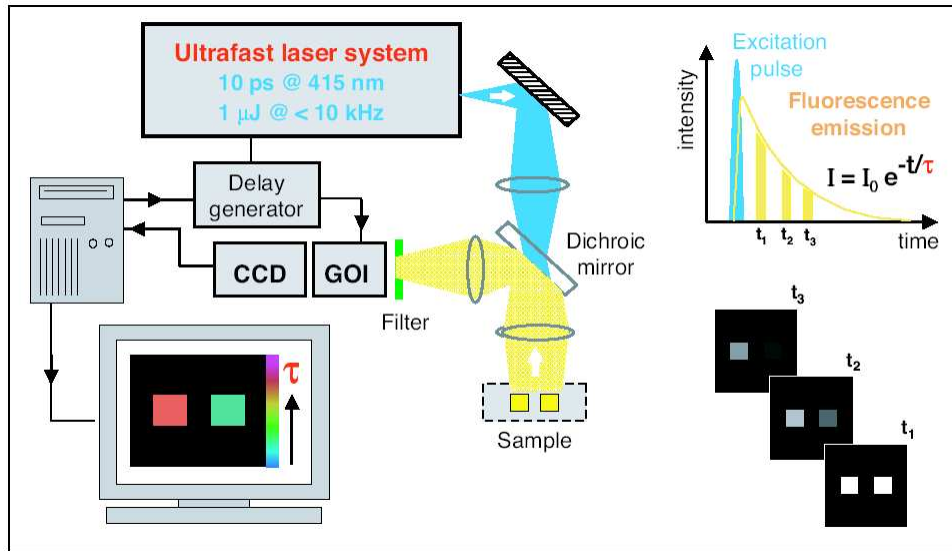


- In PALM, small sets of photoactivable fluorescent protein (PA-FP) that are attached to the protein of interest are photoactivated selectively and then bleached.
- A small area of the molecule is imaged at a time.
- The process is repeated many times until all the PA-FP have been activated and bleached.
- Using an estimated point spread function (PSF) of the microscope, the blurred image is deconvolved and replaced with a point source resulting in a very high resolution image.

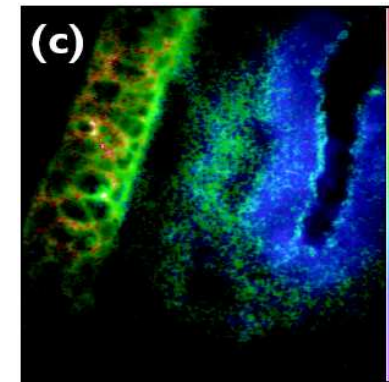
(Reproduced from [21] Betzig *et al.*, “Science”, Vol. 313, 1642-1645, 2006)

Fluorescence Lifetime Imaging Microscopy (FLIM)

[22, 23]



FLIM experiment



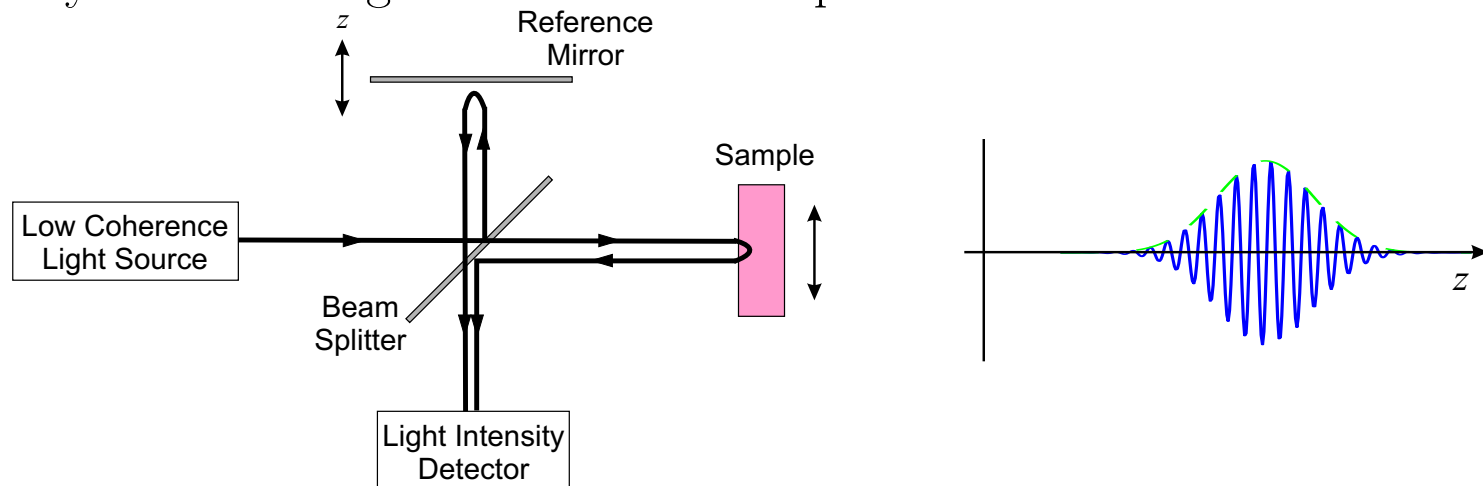
**FLIM image of
rat ear autofluorescence**

- Time- or frequency-resolved fluorescence is recorded, and decay rate is represented as an image
- Tunable mode-locked laser and gated image intensifier can be used
- Fluorescent lifetime may provide information about tissue [24]

(Reproduced from [22] Paul French group, *Opt. Phot. News*, 2002)

Optical Coherence Tomography (OCT) [25]

- 2-D or 3-D image is made by using interferometric measurement of optical backreflection or backscattering from internal tissue microstructures
- Similar in principal to RADAR ranging with optical signal
- Negligible scatter assumed
- Typically used to image tissue at small depths

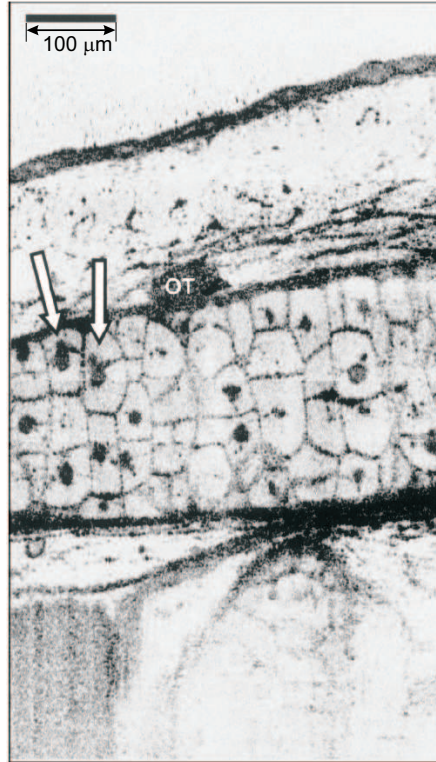


- z -direction moving of reference mirror \rightarrow longitudinal scan
- Beam moving on sample \rightarrow transverse scan
- Usually implemented with fiber optic

(Reproduced from [25] Fujimoto Group, *Science*, 1991)

OCT: Example Image [26]

- Cellular-level image of a living African frog (*Xenopus laevis*) tadpole

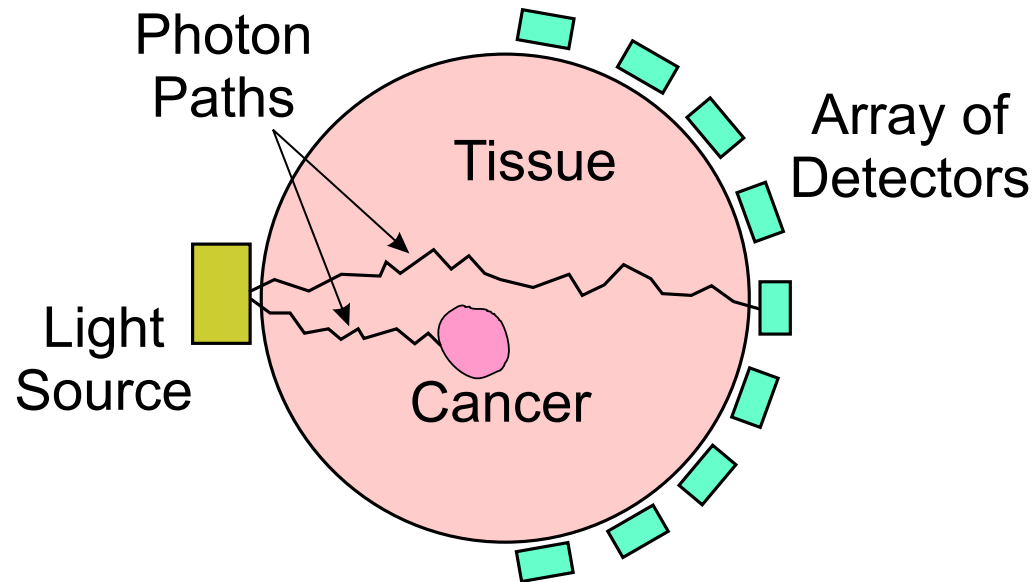


- *In vivo* subcellular level resolution: $1\ \mu\text{m} \times 3\ \mu\text{m}$ (longitudinal \times transverse)

(Reproduced from [26] W. Drexler *et al.* in Fujimoto Group, *Optics Letters*, 1999)

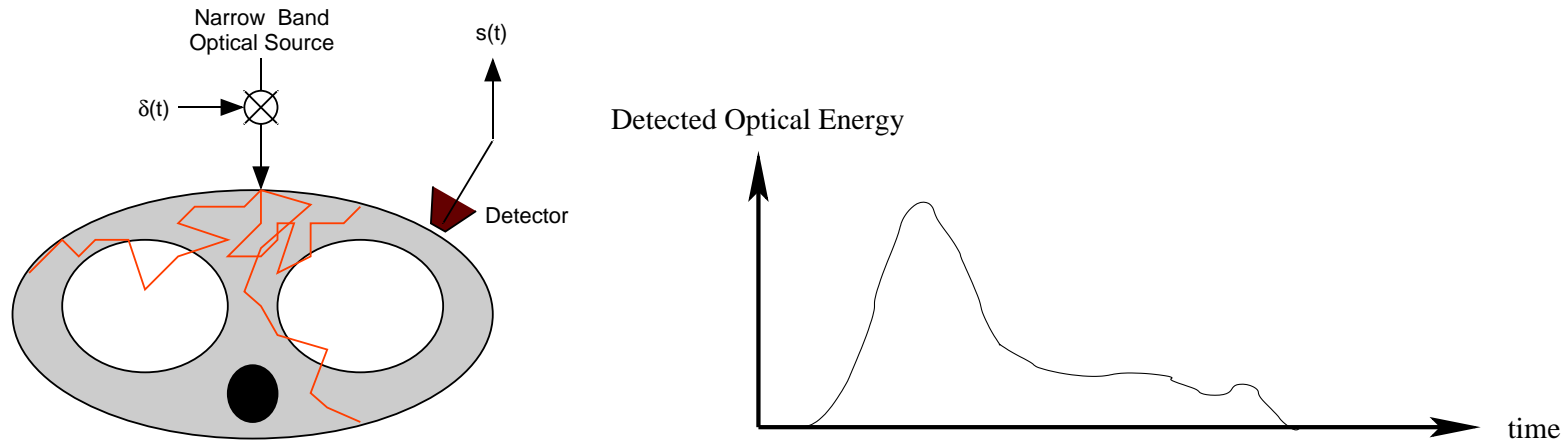
Optical Diffusion Tomography (ODT) [3]

- Measure light that passes through a highly scattering medium
- Determine unknown absorption and/or diffusion cross-section of material



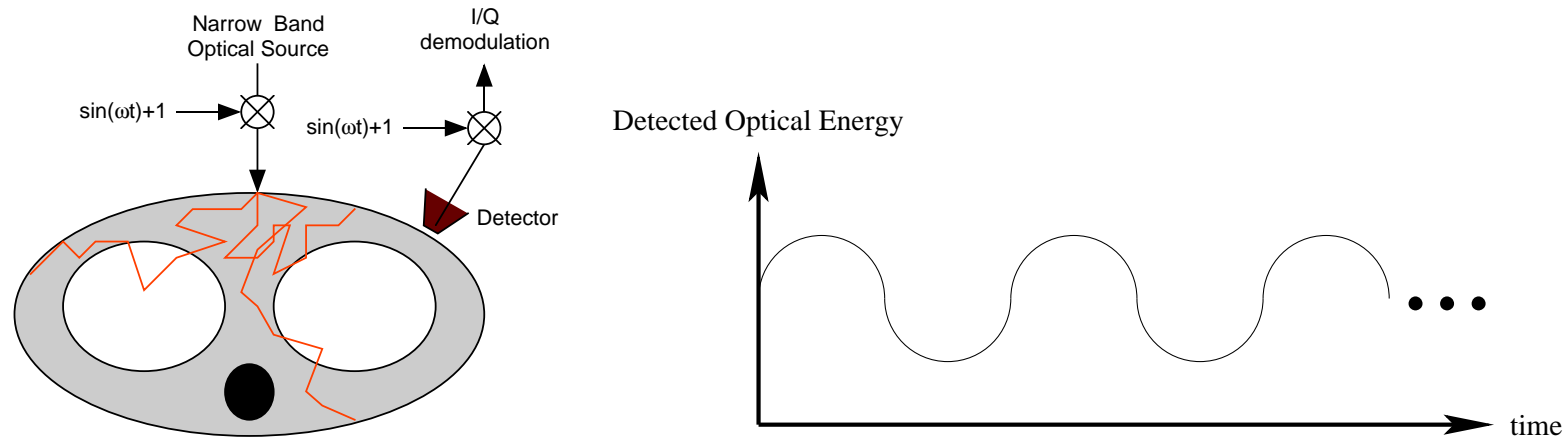
- With K sources and M detectors, there can be KM measurements
- Time domain: Measure delay of light pulse at detector
- Frequency domain: Measure amplitude/phase of modulated light envelope
- Also called “Diffuse Optical Tomography” and “Photon Migration”

ODT: Time Domain Measurements [27, 28]



- Short pulse of light at optical source input
- Light travels to detector along different paths due to scattering
- Measure time domain response, $s(t)$, at optical detector

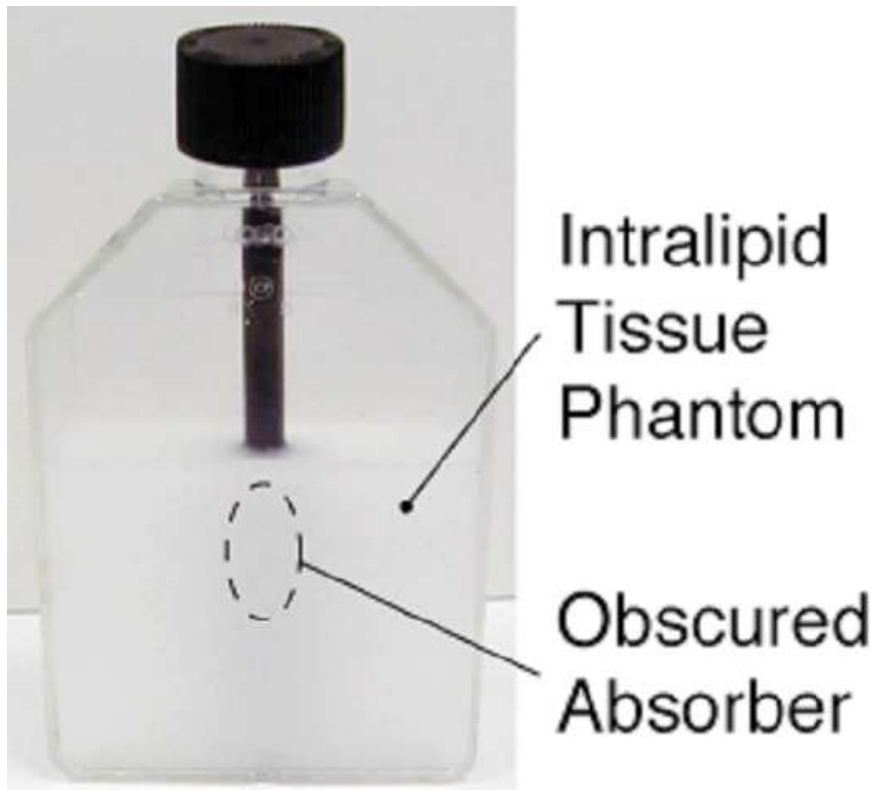
ODT: Frequency Domain Measurements



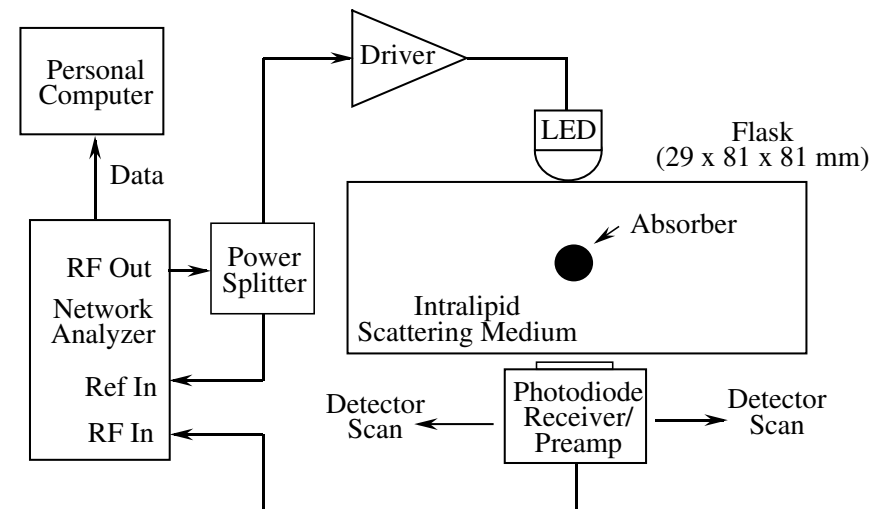
- Modulate light amplitude using RF source at frequency ω
- Measure magnitude and phase of optical detector's signal
- Scattering and absorption change magnitude and phase of detected signal
- Each measurement is a complex number
- Special case: If $\omega = 0$, this is known as continuous wave (CW) measurement

ODT Example[29, 30]: Experiment

- Intralipid solution (0.4%) solution in a 2.9 cm \times 8.1 cm \times 8.1 cm flask containing a 0.7 cm black plastic cylinder.



- Experimental apparatus
 - Near infrared LED (890nm) modulated at 10, 46, and 81 MHz
 - 2 light source positions (front and back) each with 25 detector locations

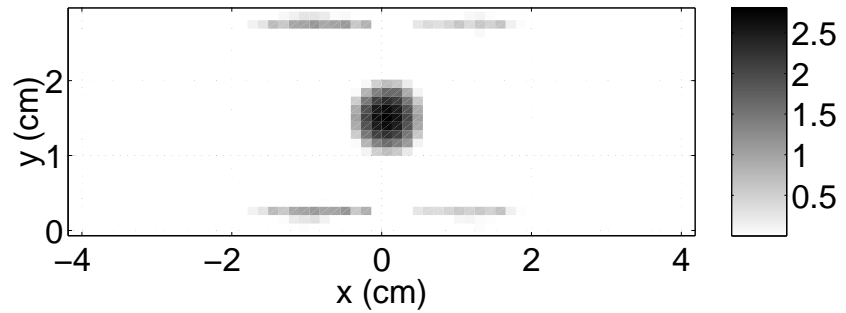
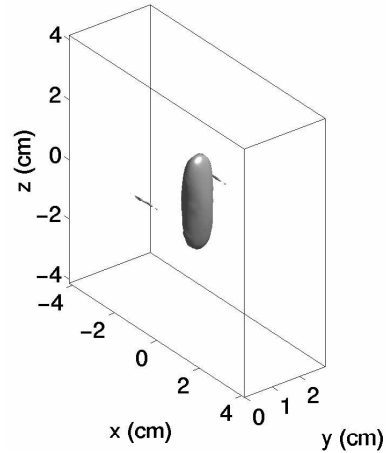


ODT: Image Reconstruction

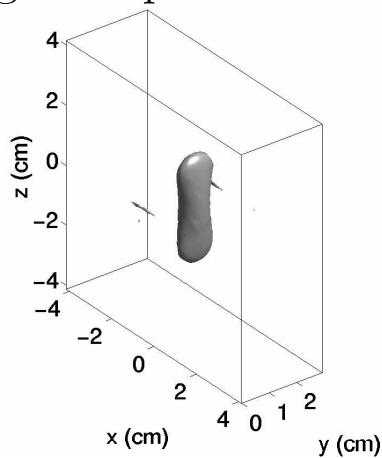
- How do you reconstruct an Image?
- It is not ...
 - Obvious
 - Easy
 - Linear
 - Filtered back projection
- But, it can be done...

ODT Example[31]: 3-D Reconstructions

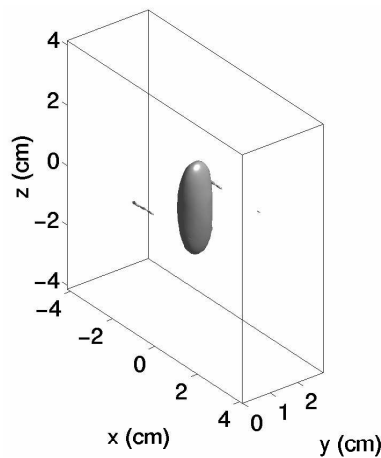
- All frequencies



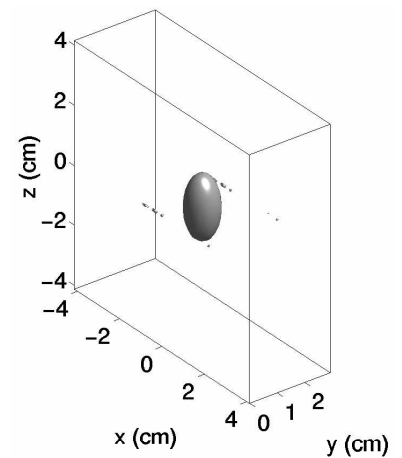
- Single frequencies



10 MHz



46 MHz

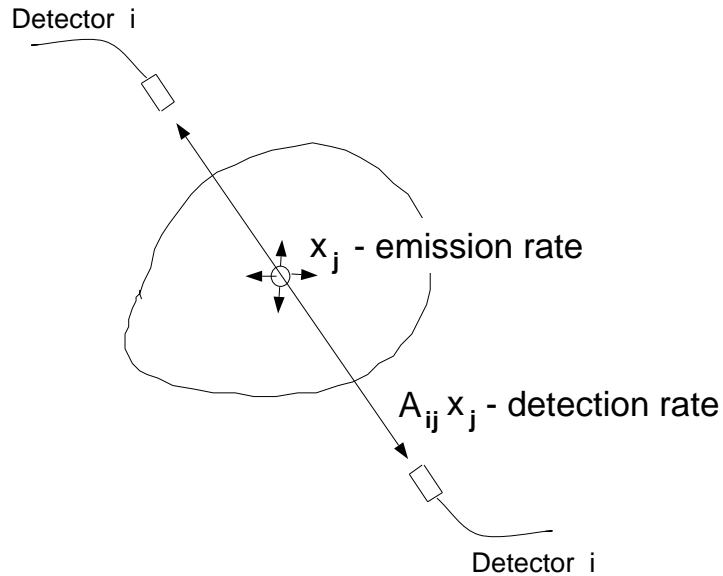


81 MHz

Milstein, Oh, Reynolds, Webb, Bouman, and Millane, *Optics Letters*, vol. 27, Jan. 2002.

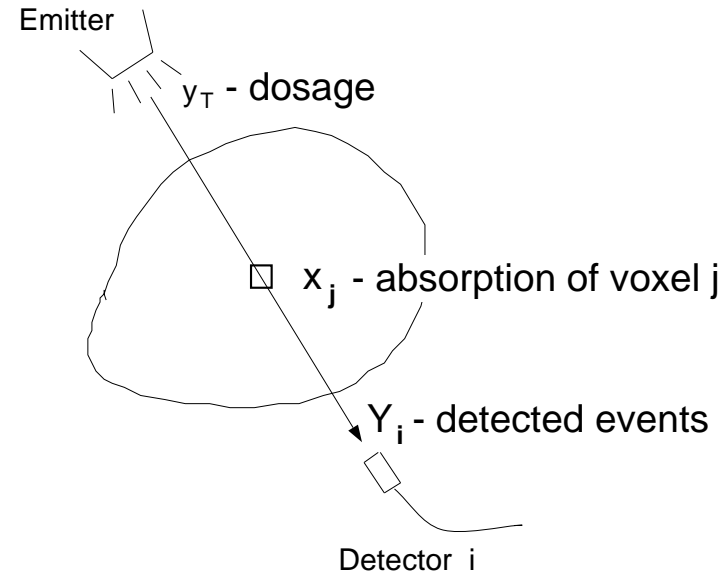
ODT: A Look at Conventional Tomography

Emission Problem



$$E[y_i] = A_{i*}x$$

Transmission Problem



$$E[y_i] = e^{-A_{i*}x} y_T$$
$$-\log \left(\frac{E[y_i]}{y_T} \right) = A_{i*}x$$

- Photons travel in a straight line
- Measurements are linearly related to unknown x
- Reconstruction is essentially matrix inversion

ODT: Contrasting ODT and Conventional Tomography

- The imaged medium determines the photons:
 - Path length distribution
 - Attenuation
 - Delay (phase)
- Forward problem:
 - Nonlinear
 - 3-dimensional
 - Modeled by partial differential equation (PDE)
 - Number of voxels \gg number of measurements
- Inverse problem:
 - Filtered back projection is inappropriate
 - Nonlinear
 - Computationally expensive

ODT: Specificity

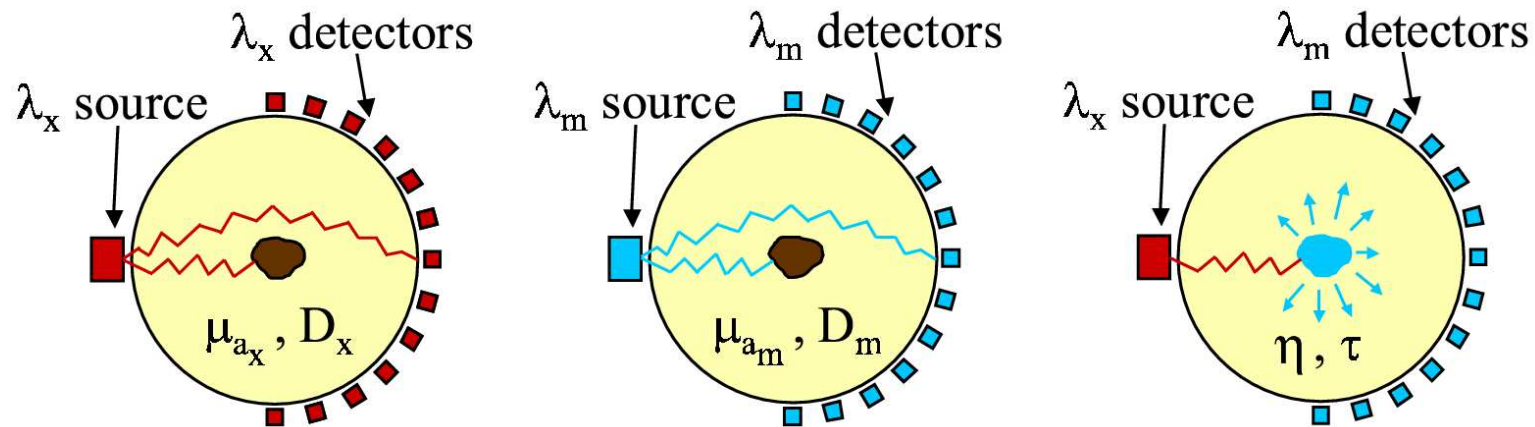
- Volumetric spectroscopy: Measure the optical properties of each voxel at each spectral wavelength
- Chemical specificity: Determine specific chemical properties through techniques such as Raman spectroscopy
- Fluorescent agents: Use near IR or visible fluorescent tracers to enhance contrast
- Fluorescent life-time imaging: Time-decay properties of fluorescent signal provide information
- Functional imaging: Measure dynamic properties of tracer uptake for applications such as pharmacokinetics
- Molecular imaging: Develop fluorescent tracers that are designed to probe specific molecular properties and target particular tissues (e.g., tumors)

ODT: Other Potential Advantages

- Safety: No radioactive exposure
- Portable: Does not require large magnet or gamma camera
- Fast: Can potentially achieve high frame rates compared to PET or MRI
- Inexpensive: Does not require coherent light
- Spatial resolution
 - Needs to be high enough to separate tissues of interest
 - Does not have resolution of CT or MRI
 - Seems reasonable to expect $\approx 1\text{mm}$ resolution $\approx 1\text{-}10\text{ cm}$ depth

Fluorescence ODT (FODT)[32]

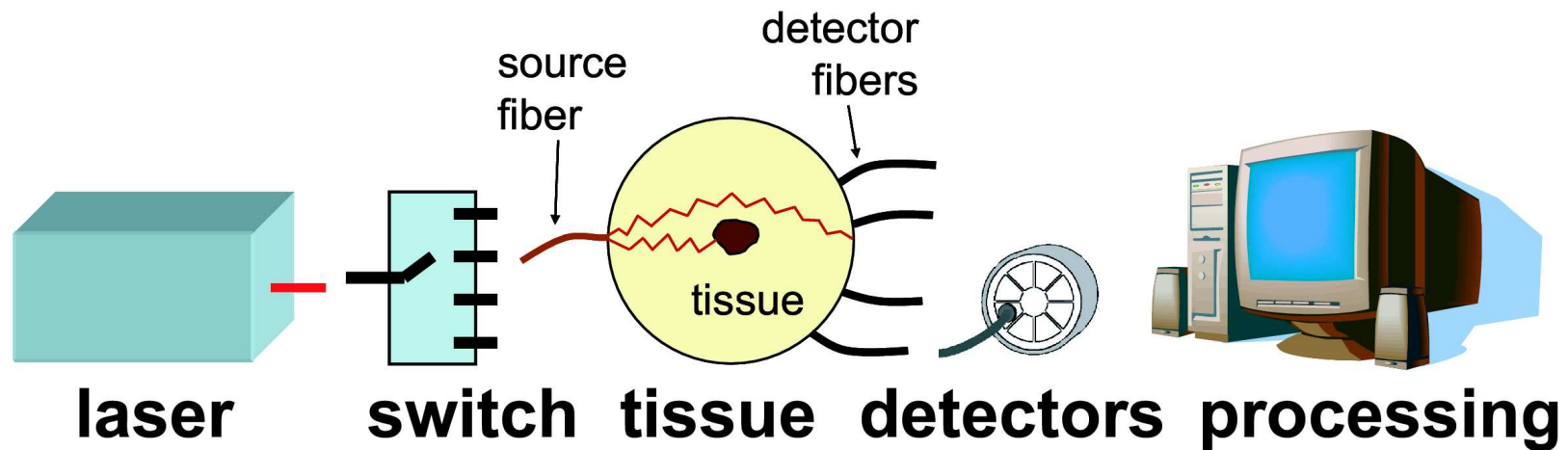
- Basic concept fluorescent tagging
 - Fluorophore provides enhanced contrast
 - With targeted delivery \rightarrow site-specific imaging (e.g. tumors)
 - Fluorophore absorbs energy at excitation wavelength, λ_x
 - Fluorophore re-emits at emission wavelength, λ_m



- Possible measurement scenarios
 - Source at λ_x and detect at $\lambda_x \Rightarrow$ ODT model
 - Source at λ_m and detect at $\lambda_m \Rightarrow$ ODT model
 - Source at λ_x and detect at $\lambda_m \Rightarrow$ Coupled ODT model

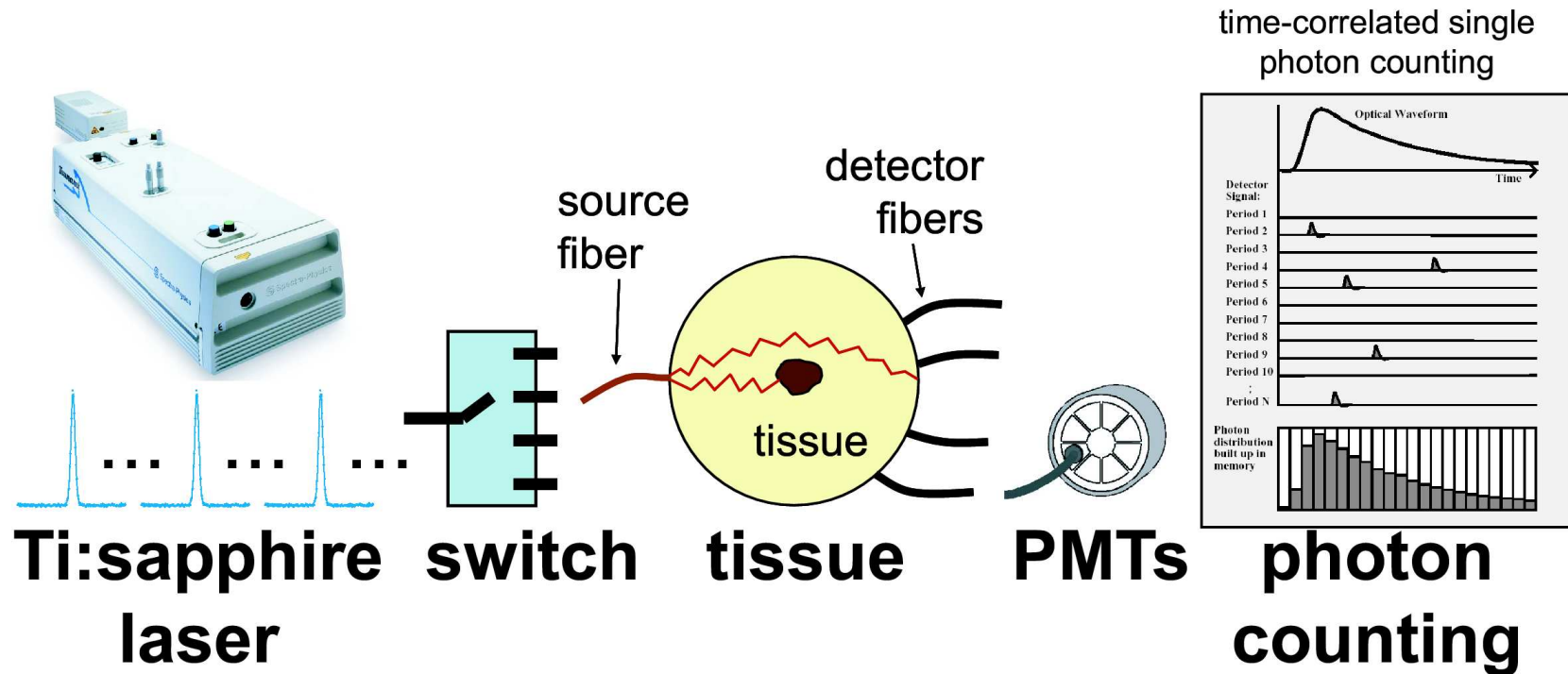
A. B. Milstein, *et al.*, “Fluorescence Optical Diffusion Tomography”, *Applied Optics*, 2003.

ODT Systems: General Components



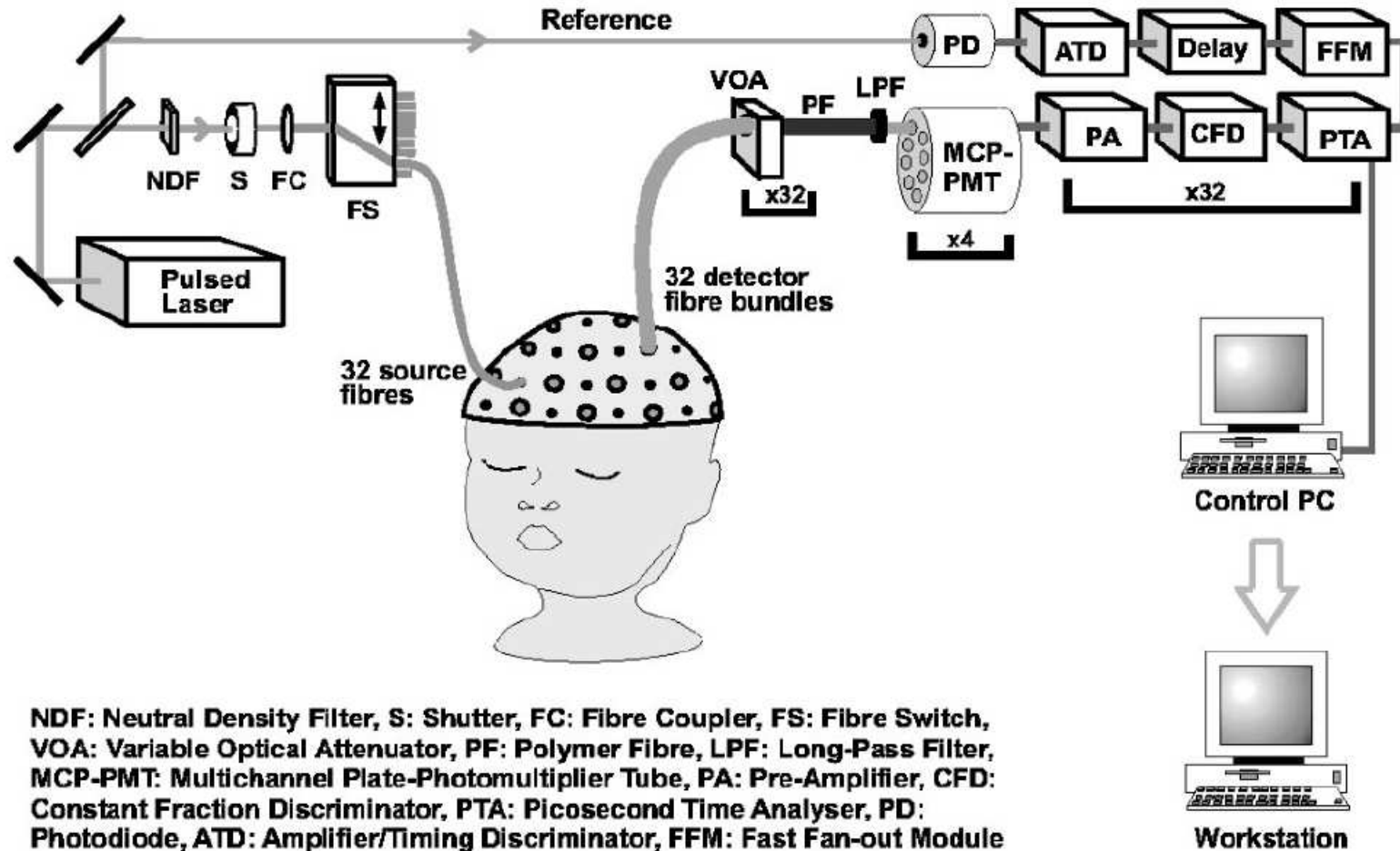
- Sources: solid state lasers, diode lasers, LEDs
- Detectors: photomultiplier tubes (PMTs), avalanche photodiodes (APDs), photodiodes (PIN), and intensified CCD cameras
- Cost and performance trade-offs (\$50 - \$250)

ODT Systems: Time Domain Overview [33, 34]



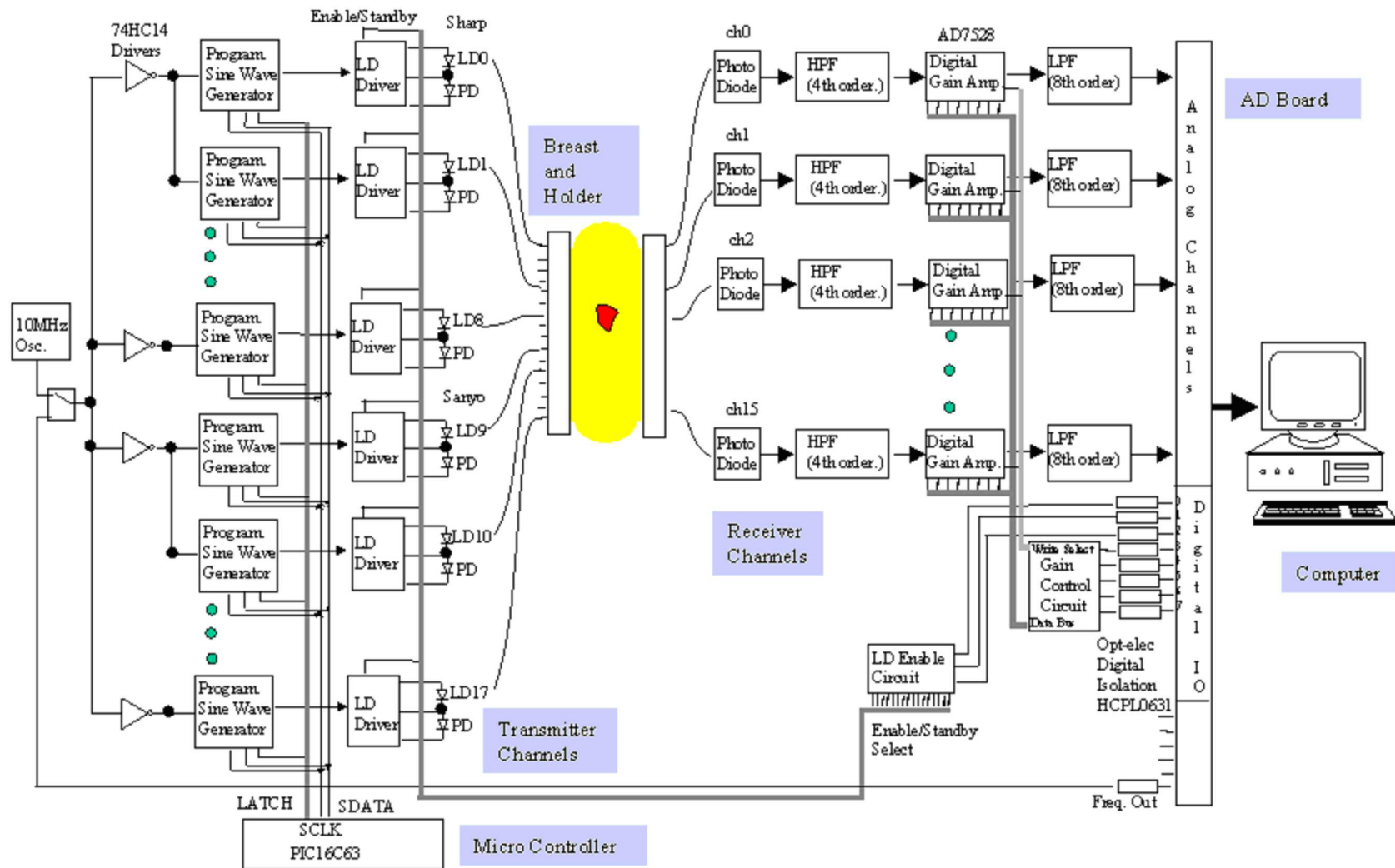
- Ti:sapphire laser pulsed with 80 MHz repetition rate
- Time-correlated single photon counting: individual photons are counted for delay times relative to trigger pulses

ODT Systems: Time Domain: UCL Imager [33]



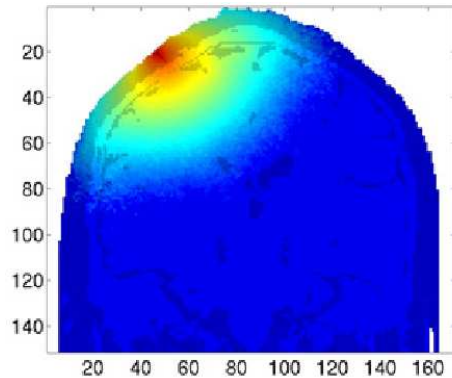
(Reproduced from Schmidt *et al.*, *Rev. Sci. Inst.*, 2000)

ODT Systems: Continuous-Wave (CW): MGH Imager [35]

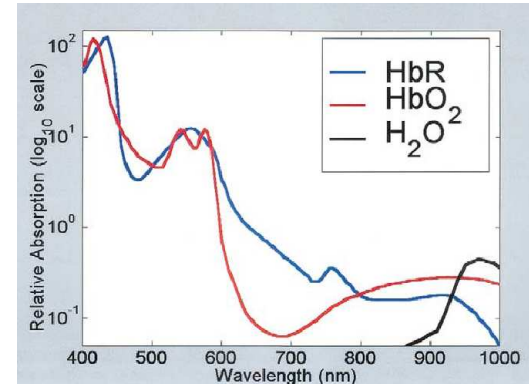


(Reproduced from Zhang *et al.*, *Proc. SPIE*, 2001)

Applications: Functional Brain Imaging [36, 37]



Simulation of light entering brain[37]

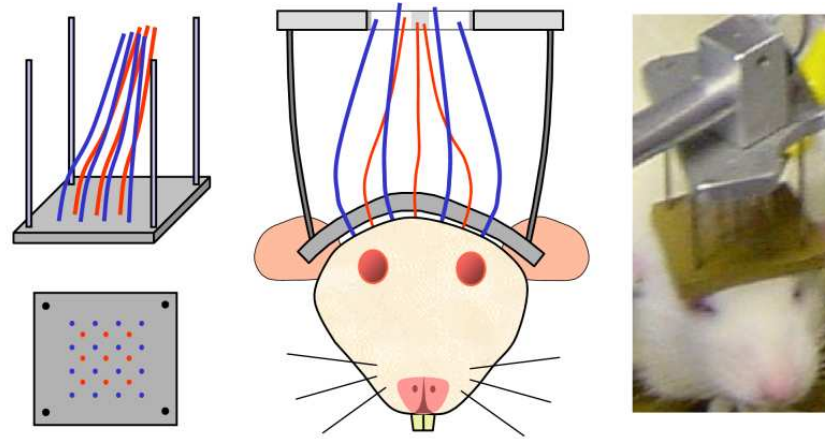


HbO₂ and HbR absorption[36]

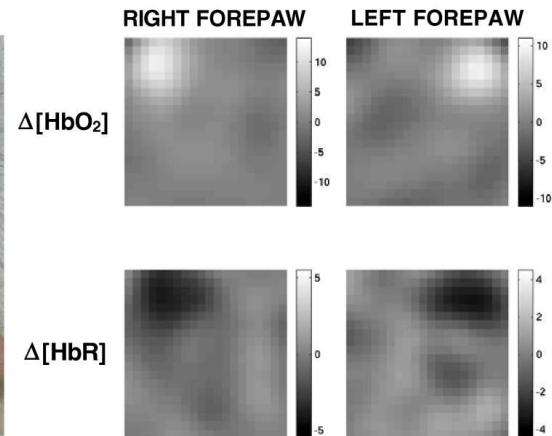
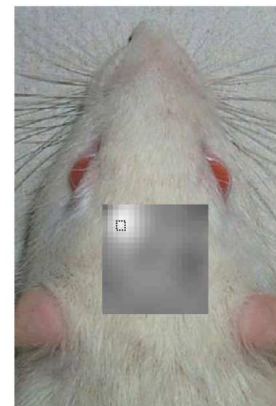
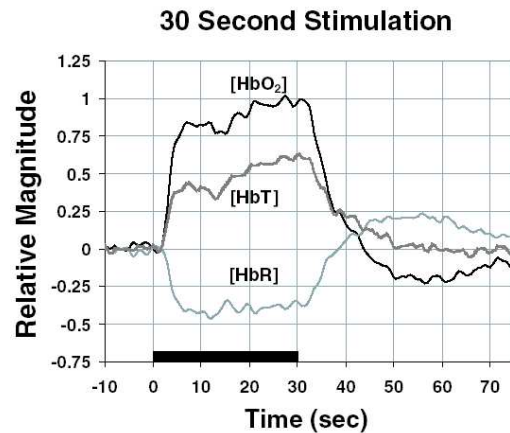
- NIR light can penetrate through the human skull into the brain
- Local changes in oxyhemoglobin ([HbO₂]) and deoxyhemoglobin ([HbR]) concentration indicate brain activity
- ODT can quantify [HbO₂] and [HbR] in the brain due to absorption at different optical wavelengths
- Optical methods can have higher temporal resolution than BOLD fMRI, but lower spatial resolution

(Reproduced from [36] Strangman *et al.*, *Biol. Psych.*, 2002, and [37] Boas *et al.*, *Opt. Exp.*, 2002)

Applications: Hemodynamics in Rat Subject[38]



Fiber optic probe measures brain while
forepaws electrically stimulated



Hemodynamic response

$\Delta[\text{HbO}_2]$ and $\Delta[\text{HbR}]$ images

(Reproduced from Siegel *et al.*, *Phys. Med. Biol.*, 2003)

Applications: 3D Hemodynamics in Humans[39]



Commercial instrument[40, 41] measures brain during breathing exercise

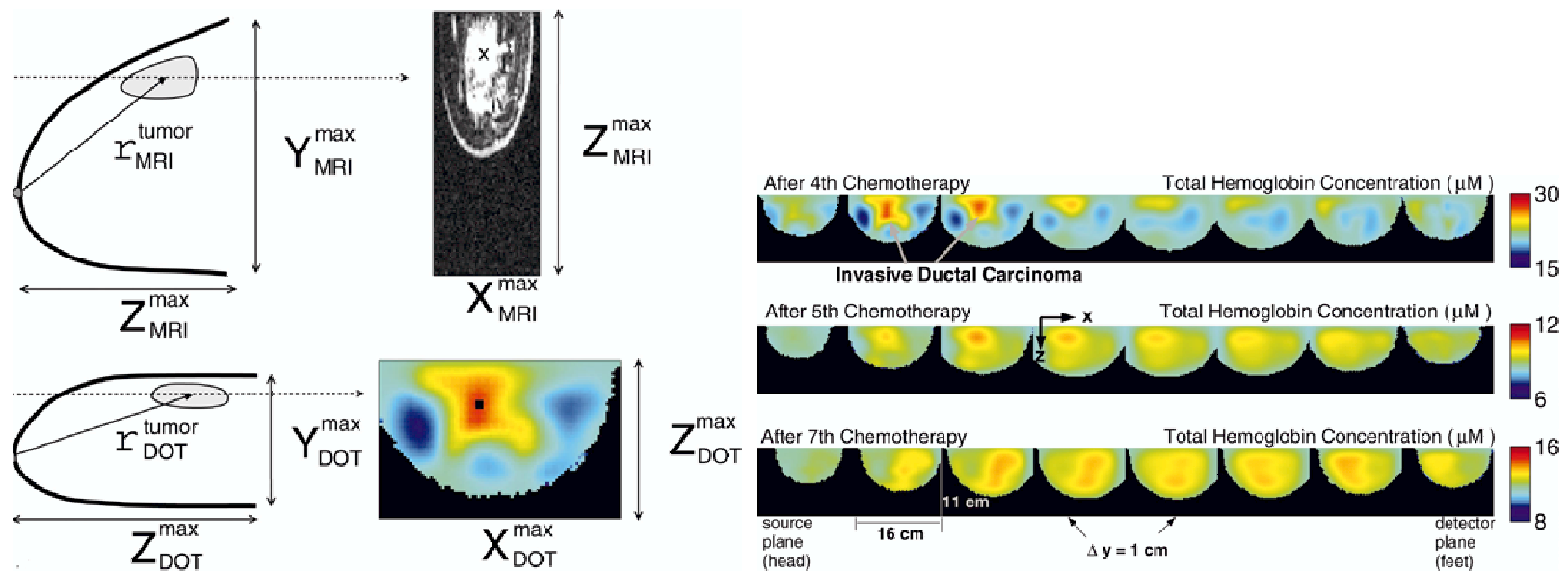


$\Delta([\text{HbO}_2] + [\text{HbR}])$ images

$\Delta[\text{HbO}_2]$ images

(Reproduced from Bluestone *et al.*, *Opt. Exp.*, 2001, and NIRx Medical Technologies website)

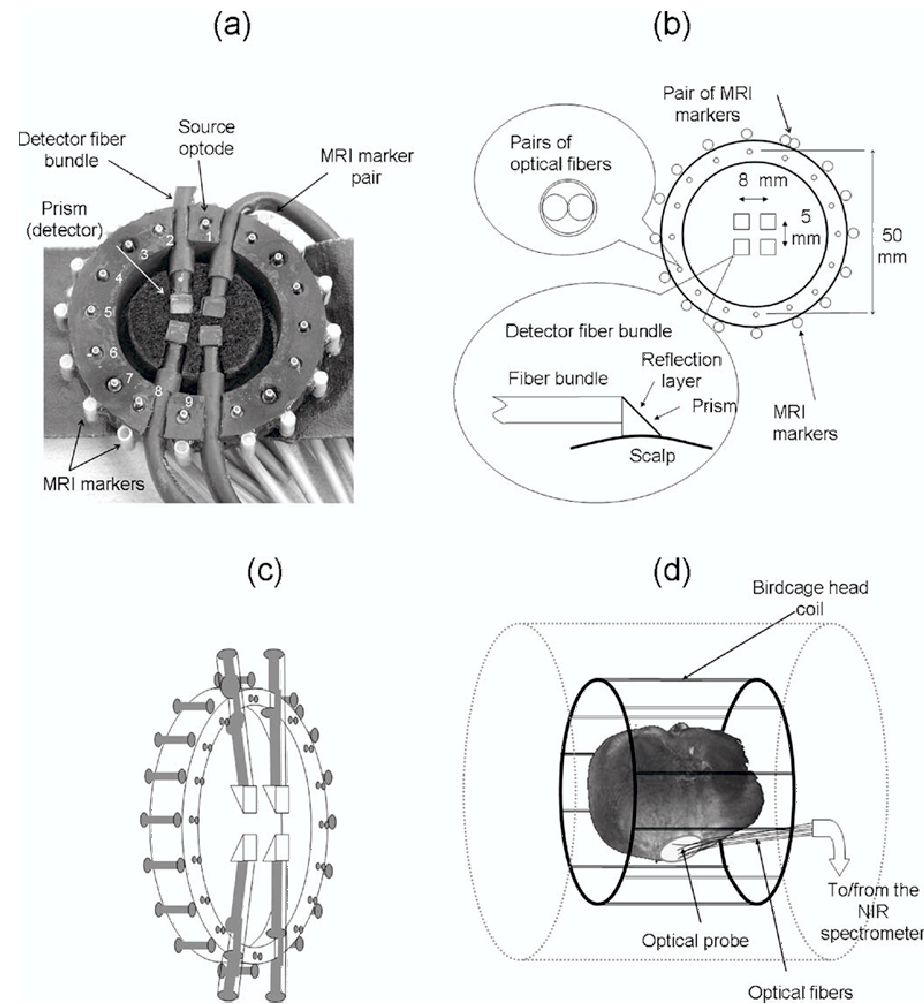
ODT Application: Chemotherapy Monitoring [42]



- ODT was used for tracking the progress of a female patient with breast cancer during neoadjuvant chemotherapy.
- The reconstructed hemoglobin concentration after each chemotherapy session shows a decrease in the size of tumor.
- The ODT reconstructed breast image is compared to an MRI image.

(Reproduced from [42] Choe *et al.*, *Med. Phys.*, vol. 32 (4), pp. 1128-1139, 2005)

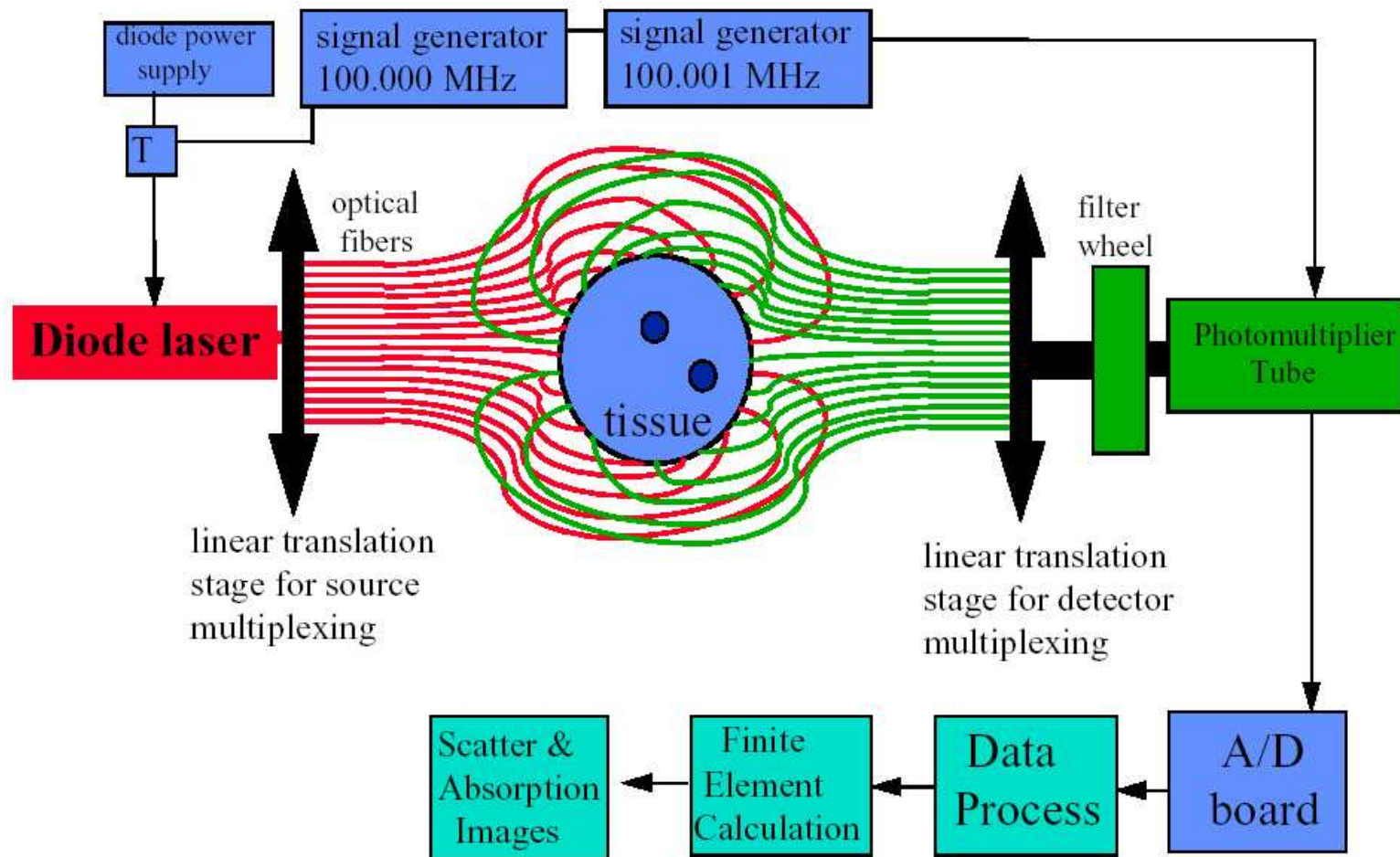
ODT Application: ODT Combined with MRI [43]



- Integrated measurement system for simultaneous functional MRI and ODT imaging of hemodynamics in human brain

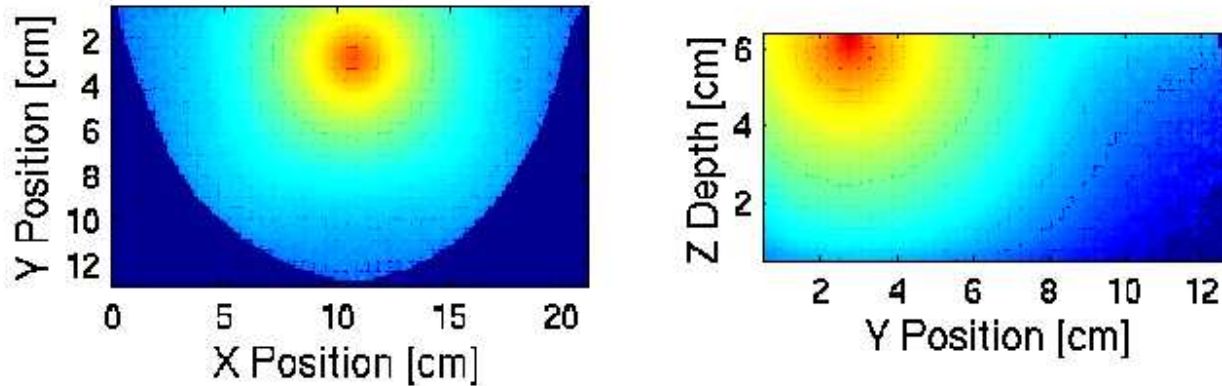
(Reproduced from [43] Zhang *et al.*, *Rev. Sci. Instr.*, 77, 114301, 2006)

ODT Systems: Frequency Domain: Dartmouth Imager [44]



(Reproduced from Pogue *et al.*, *Opt. Exp.*, 1997)

Applications: Breast Imaging



Simulation of light in breast [45]

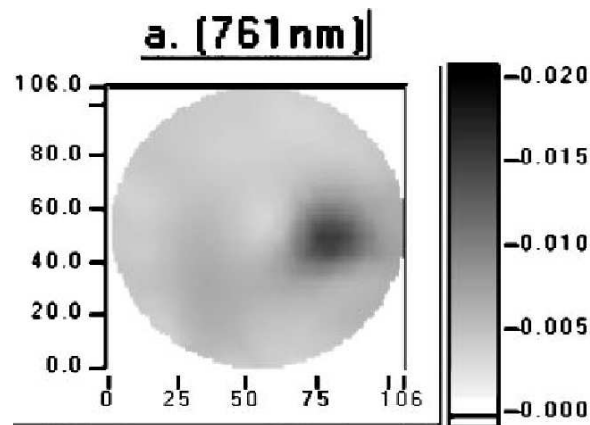
- Currently, X-ray mammography detects structural changes in tumors compared to surrounding tissue
- Breast tumors tend to have higher absorption than surrounding tissue due to increased vascular density
- Optical methods potentially will offer earlier diagnosis by observing changes in absorption before structural changes take place

(Reproduced from Stott, MGH presentation, 2002.)

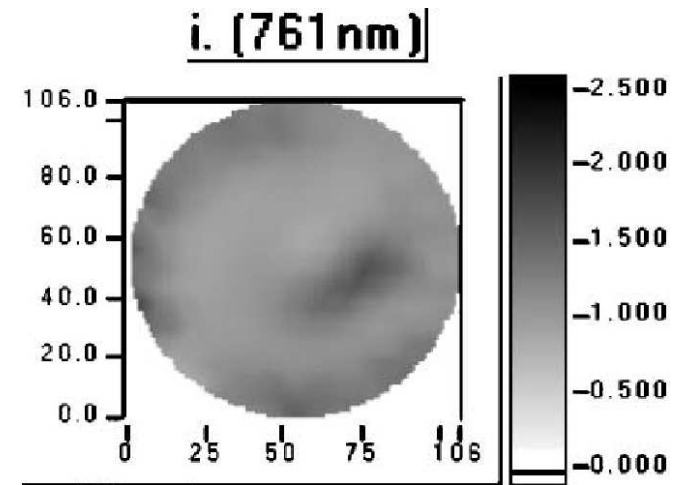
Applications: Breast Tumor Measurements [46]



Measurement table and instrument used at Dartmouth



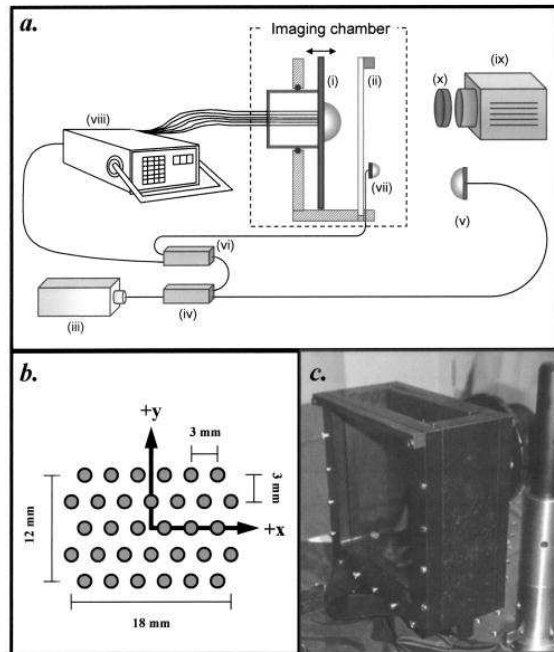
Breast absorption



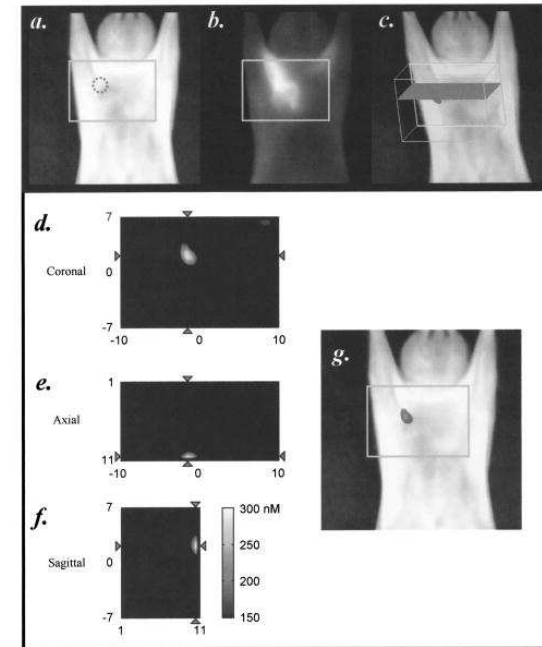
Breast scatter

(Reproduced from McBride *et al.*, *J. Biomed. Opt.*, 2002)

Fluorescence Molecular Tomography for Small Animal Imaging [47]



FMT system

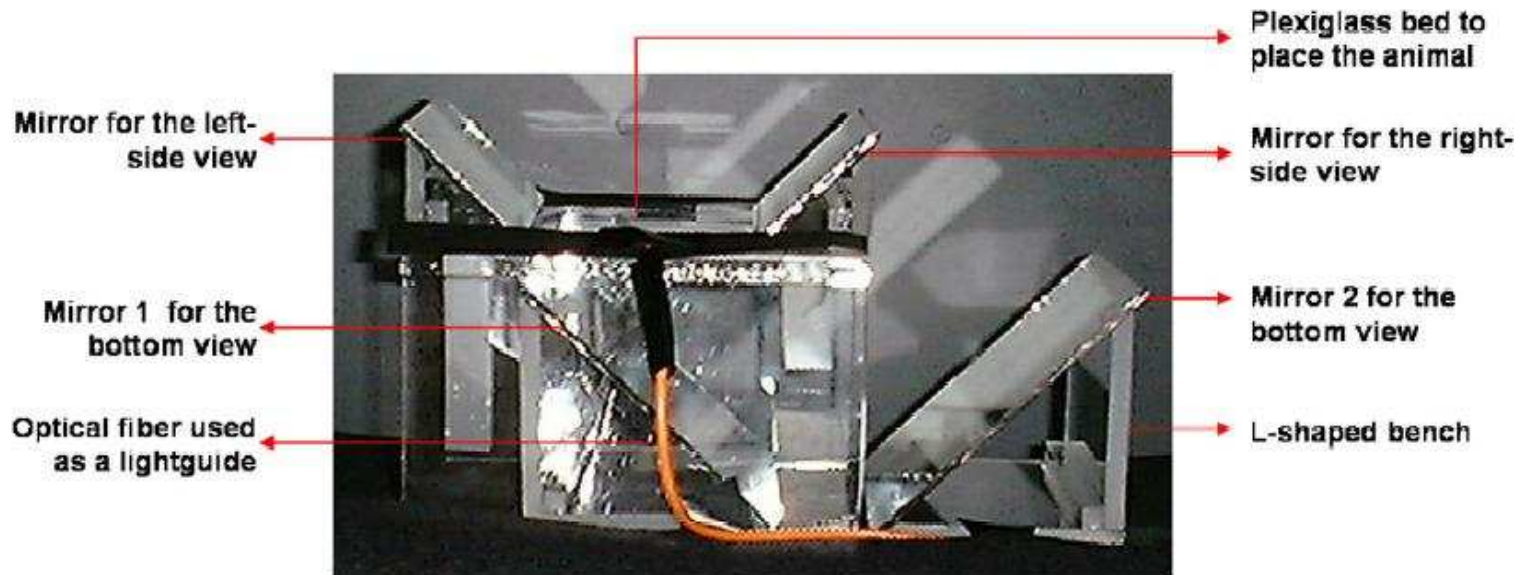


In vivo fluorescence reflectance and tomographic imaging

- Fluorochrome distribution and concentration are reconstructed
- Submillimeter resolution is reported
- A similar system is also used for fluorescent protein tomography [48]

(Reproduced from [47] E. Graves *et al.*, *Med. Phys.*, 2003)

Bioluminescence Optical Tomography for Small Animal Imaging [49]

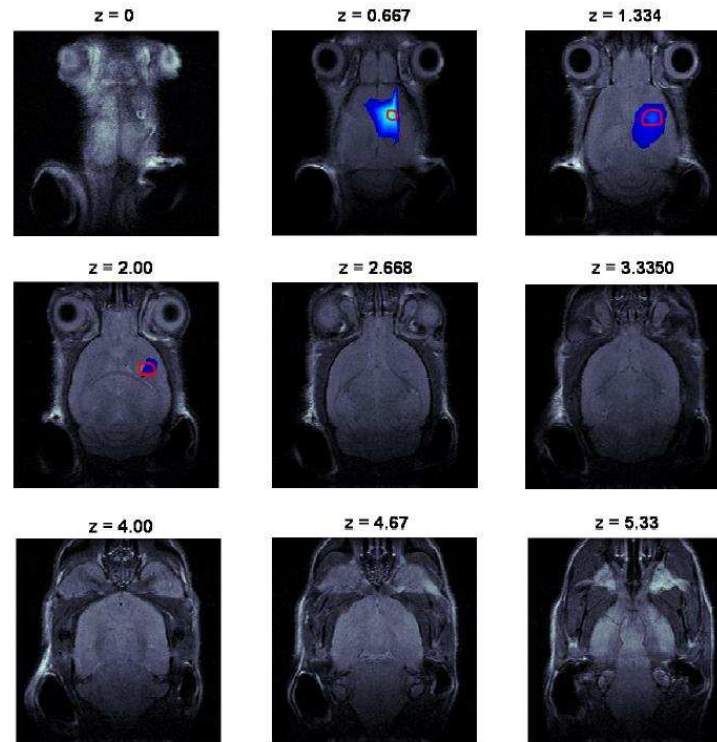


BLT system

- The first 3D *in vivo* bioluminescence tomography system
- The set-up has no moving parts. A CCD camera is placed on the top.
- Hyperspectral and multispectral measurement data are used
- MicroCT scanner is used anatomic information

(Reproduced from [49] A. Chaudhari *et al.*, *Phys. Med. Bio.*, 2005)

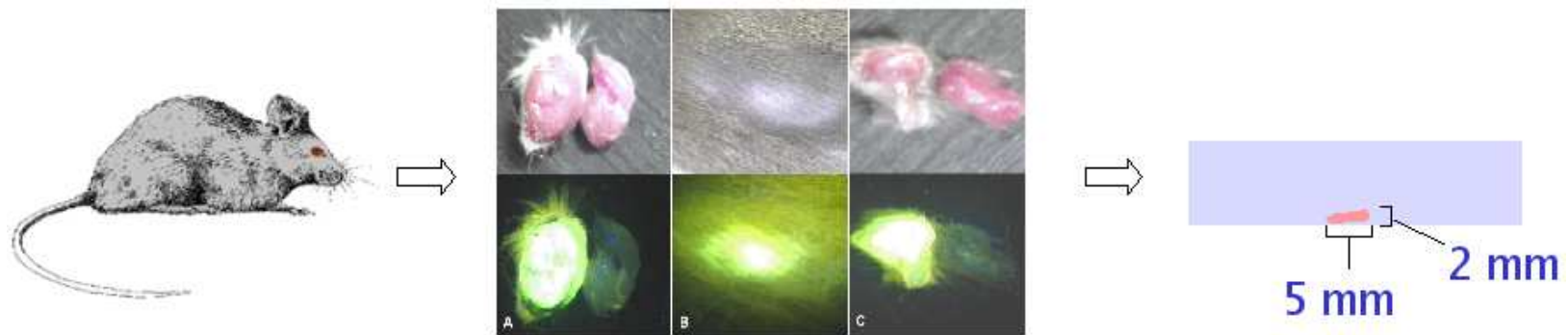
Bioluminescence Optical Tomography for Small Animal Imaging [49]



Reconstructed bioluminescence data are overlaid on co-registered MR slices. The red contour indicates the boundary of the implanted brain tumor.

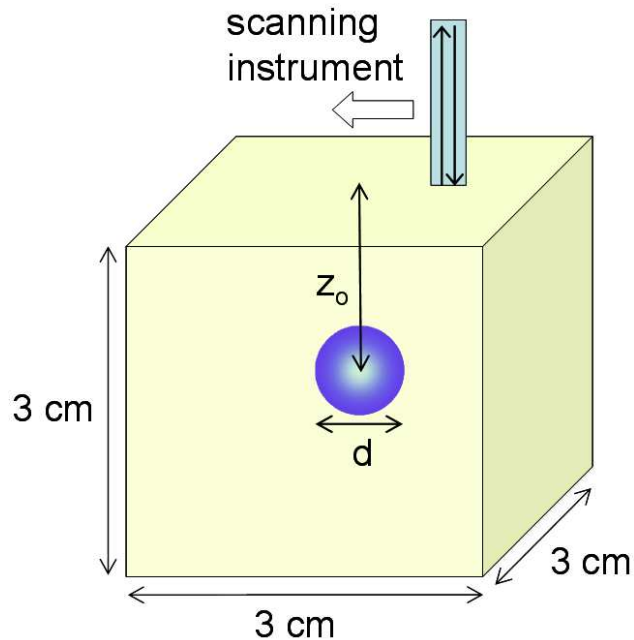
(Reproduced from [49] A. Chaudhari *et al.*, *Phys. Med. Bio.*, 2005)

Folate Targeting: Mouse Tumors Grown[18]



- Mouse induced to grow lung tumor and injected with 10 nmols of folate-fluorescein
- Portion of tumor excised and frozen for later experimental use
- Before measurement, tumor thawed and glued to Petri dish

Folate Targeting: Simulation Geometry



- Concept: a fiber optic probe incorporated into a surgical instrument
- Patient injected with targeted fluorescent contrast agent
- Two fibers for fluorescent measurement: excitation and collection
- Scan measurement and mathematical model allow reconstruction of tumor position

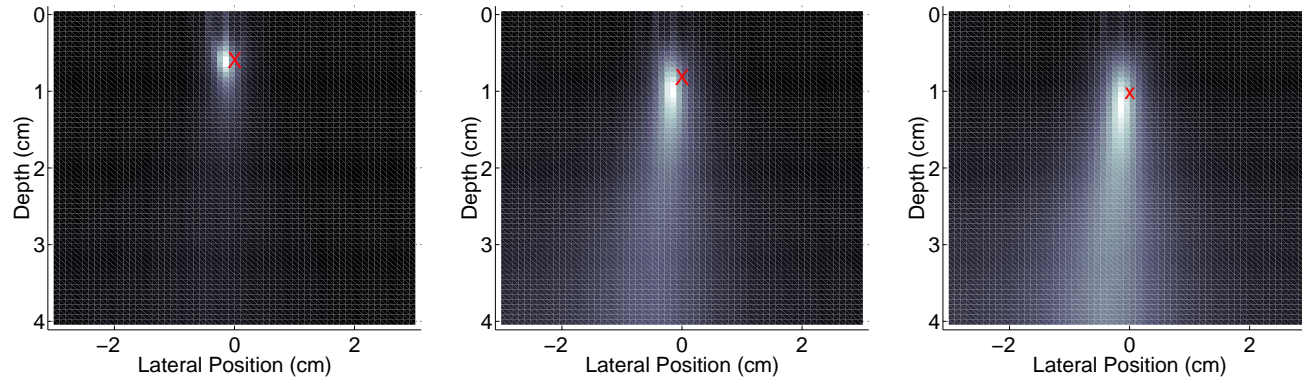
Folate Targeting: Tumor Localization: Fit to Model

- Tumor position estimated by fitting measurements to diffusion model
- Computational domain with $65 \times 65 \times 65$ volume elements simulates volume of size $6 \text{ cm} \times 6 \text{ cm} \times 4 \text{ cm}$
- Assumption: $\mu_a = 0 \text{ cm}^{-1}$, $\mu'_s = 1/3D = 15 \text{ cm}^{-1}$

$$\mathbf{r}^* = \arg \min_{\mathbf{r}} c(\mathbf{r})$$
$$c(\mathbf{r}) = \min_w \left\{ \sum_{k=1}^K \frac{[y_k - w f_k(\mathbf{r})]^2}{y_k} \right\},$$

- \mathbf{r}^* : estimated tumor position
 $f_k(\mathbf{r})$: computed data for k^{th} scan position and point source tumor at \mathbf{r}
 y_k : k^{th} measurement in scan
 w : normalizing weight

Folate Targeting: Results



- $\log c(\mathbf{r})$ plots show estimated tumor position
- Uncertainty in estimate increases with depth
- Despite limited data, horizontal and vertical positions recovered accurately within 2.1 mm

References

- [1] R. M. P. Doornbos, R. Lang, M. C. Aalders, F. W. Cross, and H. J. C. M. Sterenborg, “The determination of *in vivo* human tissue optical properties and absolute chromophore concentrations using spatially resolved steady-state diffuse reflectance spectroscopy,” *Phys. Med. Biol.*, vol. 44, pp. 967–981, 1999.
- [2] F. F. Jobsis, “Noninvasive, infrared monitoring of cerebral and myocardial oxygen sufficiency and circulatory parameters,” *Science*, vol. 198, pp. 1264–1267, 1977.
- [3] S. R. Arridge, “Optical tomography in medical imaging,” *Inverse Problems*, vol. 15, pp. R41–R93, 1999.
- [4] G. Godin, J.-A. Beraldin, M. Rioux, M. Levoy, L. Cournoyer, and F. Blais, “An assessment of laser range measurement of marble surfaces,” *Proceedings of the 5th Conference on Optical 3-D Measurement Techniques*, October 1-4 2001, Vienna, Austria.
- [5] A. E. Siegman, *Lasers*. University Science Books, 1986.
- [6] V. Ntziachristos, A. G. Yodh, M. Schnall, and B. Chance, “Concurrent MRI and diffuse optical tomography of breast after indocyanine green enhancement,” *Proc. Natl. Acad. Sci.*, vol. 97, no. 6, pp. 2767–2772, March 14 2000.
- [7] S. Mathieu and A. El-Battari, “Monitoring e-selectin-mediated adhesion using green and red fluorescent proteins,” *Journal of Immunological Methods*, vol. 272, pp. 81–92, 2003.
- [8] S. Bhaumik and S. S. Gambhir, “Optical imaging of renilla luciferase reporter gene expression in living mice,” *Proc. Natl. Acad. Sci. USA*, vol. 99, no. 1, pp. 377–382, 2002.
- [9] C. V. Raman and K. S. Krishnan, “A new type of secondary radiation,” *Nature*, vol. 121, no. 3048, p. 501, March 1928.
- [10] J. R. Ferraro, K. Nakamoto, and C. W. Brown, *Introduction to Raman Spectroscopy*. Academic Press, 2003.
- [11] C. A. Thompson, J. S. R. K. J. Webb, F. P. LaPlant, and D. Ben-Amotz, “Raman spectroscopic studies of diamond in Intralipid,” *Optics Letters*, vol. 20, no. 10, pp. 1195–1197, May 15 1995.
- [12] A. J. Berger, T.-W. Koo, I. Itzkan, G. Horowitz, and M. S. Feld, “Multicomponent blood analysis by near-infrared raman spectroscopy,” *Applied Optics*, vol. 38, no. 13, p. 2916, May 1999.
- [13] M. V. Knopp, E. Weiss, H. P. Sinn, J. Mattern, H. Junkermann, J. Radeleff, A. Magener, G. Brix, S. D. S. I. Zuna, and G. van Kaick, “Pathophysiologic basis of contrast enhancement in breast tumors,” *Journal of Magnetic Resonance Imaging*, vol. 10, no. 3, pp. 260–266, 1999.

- [14] P. J. Hudson, "Recombinant antibodies: a novel approach to cancer diagnosis and therapy," *Expert Opinion on Investigational Drugs*, vol. 9, no. 6, pp. 1231–1242, 2000.
- [15] S. D. Jonson and M. J. Welch, "PET imaging of breast cancer with fluorine-18 radiolabeled estrogens and progestins," *Quarterly Journal of Nuclear Medicine*, vol. 42, no. 1, pp. 8–17, 1998.
- [16] A. Heppeler, S. Froidevaux, A. N. Eberle, and H. R. Maecke, "Receptor targeting for tumor localisation and therapy with radiopeptides," *Current Medicinal Chemistry*, vol. 7, no. 9, pp. 971–994, 2000.
- [17] J. A. Reddy and P. S. Low, "Folate-mediated targeting of therapeutic and imaging agents to cancers," *Critical Reviews in Therapeutic Drug Carrier Systems*, vol. 15, no. 6, pp. 587–627, 1998.
- [18] K. J. Webb, A. B. Milstein, M. D. Kennedy, K. N. Jallad, C. A. Bouman, D. Ben-Amotz, and P. S. Low, "Folate conjugate fluorescence labeling for tumor localization," *Third Inter-Institute Workshop on Diagnostic Optical Imaging and Spectroscopy: The Clinical Adventure. Bethesda, MD, 2002, vol Poster Presentation*, September 2002, Bethesda, MD.
- [19] X. Michalet, F. F. Pinaud, L. A. Bentolila, J. M. Tsay, S. Doose, J. J. Li, G. Sundaresan, A. M. Wu, S. S. Gambhir, and S. Weiss, "Quantum Dots for Live Cells, in Vivo Imaging, and Diagnostics," *Science*, vol. 307, no. 5709, pp. 538–544, 2005.
- [20] J. R. Mansfield, K. W. Gossage, C. C. Hoyt, and R. M. Levenson, "Autofluorescence removal, multiplexing, and automated analysis methods for in-vivo fluorescence imaging," *J. Biomed. Opt.*, vol. 10, no. 4, p. 041207, 2005.
- [21] E. Betzig, G. Patterson, R. Sougrat, O. Lindwasser, S. Olenych, J. Bonifacino, M. Davidson, J. Lippincott-Schwartz, and H. F. Hess, "Imaging intracellular fluorescent proteins at nanometer resolution," *Science*, vol. 313, pp. 1642–1645, Sept. 2006.
- [22] D. Elson, S. Webb, J. Siegel, K. Suhling, D. Davis, J. Lever, D. Philips, A. Wallace, and P. French, "Biomedical applications of fluorescence lifetime imaging," *Opt. Photon. News*, pp. 26–32, Nov. 2002.
- [23] K. Dowling, M. J. Dayel, M. J. Lever, P. M. W. French, J. D. Hares, and A. K. L. Dymoke-Bradshaw, "Fluorescence lifetime imaging with picosecond resolution for biomedical applications," *Optics Letters*, vol. 23, no. 10, pp. 810–812, May 15 1998.
- [24] S. B. Bambot, J. R. Lakowicz, and G. Rao, "Potential applications of lifetime-based, phase-modulation fluorimetry in bioprocess and clinical monitoring," *Trends Biotechnol.*, vol. 13, pp. 106–115, March 1995.
- [25] D. Huang, E. Swanson, C. Lin, J. Schuman, W. Stinson, W. Chang, M. Hee, T. Flotte, D. Gregory, C. Puliafito, and J. Fujimoto, "Optical coherence tomography," *Science*, vol. 254, pp. 1178–1181, Nov 1991.

- [26] W. Drexler, U. Morgner, F. X. Kartner, C. Pitris, S. A. Boppart, X. D. Li, E. P. Ippen, and J. G. Fujimoto, “*In vivo* ultrahigh-resolution optical coherence tomography,” *Opt. Lett.*, vol. 24, no. 17, pp. 1221–1223, Sep. 1999.
- [27] D. A. Benaron and D. K. Stevenson, “Optical time-of-flight and absorbance imaging of biologic media,” *Science*, vol. 259, no. 5100, pp. 1463–1466, 1993.
- [28] B. Chance, J. S. Leigh, H. Miyake, D. S. Smith, S. Nioka, R. Greenfeld, M. Finander, K. Kaufmann, W. Levy, and *et al.* M. Young, “Comparison of time-resolved and -unresolved measurements of deoxyhemoglobin in brain,” *Proc Natl Acad Sci U S A.*, vol. 85, no. 14, pp. 4971–4975, July 1988.
- [29] J. S. Reynolds, A. Prasadka, S. Yeung, and K. J. Webb, “Optical diffusion imaging: a comparative numerical and experimental study,” *Applied Optics*, vol. 35, no. 19, pp. 3671–3679, July 1996.
- [30] J. S. Reynolds, C. A. Thompson, K. J. Webb, F. P. LaPlant, and D. Ben-Amotz, “Frequency domain modeling of reradiation in highly scattering media,” *Applied Optics*, vol. 36, pp. 2252–2259, April 1997.
- [31] A. B. Milstein, S. Oh, J. S. Reynolds, K. J. Webb, C. A. Bouman, and R. P. Millane, “Three-dimensional Bayesian optical diffusion tomography using experimental data,” *Optics Letters*, vol. 27, pp. 95–97, January 2002.
- [32] A. B. Milstein, S. Oh, K. J. Webb, C. A. Bouman, Q. Zhang, D. A. Boas, and R. P. Millane, “Fluorescence optical diffusion tomography,” *Applied Optics*, vol. 42, no. 16, pp. 3081–3094, June 2003.
- [33] F. E. W. Schmidt, M. E. Fry, E. M. C. Hillman, J. C. Hebden, and D. T. Delpy, “A 32-channel time-resolved instrument for medical optical tomography,” *Rev. Sci. Inst.*, vol. 71, no. 1, pp. 256–265, Jan. 2000.
- [34] W. Becker, A. Bergmann, G. Biscotti, and A. Ruck, “Advanced time-correlated single photon counting techniques for spectroscopy and imaging in biomedical systems,” *Proceedings of the SPIE 5340: Commercial and Biomedical Applications of Ultrafast Lasers*, vol. 5340, January 2004, San Jose, CA.
- [35] Q. Zhang, T. J. Brukilacchio, T. Gaudett, L. Wang, A. Li, and D. A. Boas, “Experimental comparison of using continuous-wave and frequency-domain diffuse optical imaging systems to detect heterogeneities,” *Proc. SPIE*, vol. 4250, June 2001, pp. 219–238.
- [36] G. Strangman, D. A. Boas, and J. P. Sutton, “Non-invasive neuroimaging using near-infrared light,” *Biol. Psychiatry*, vol. 52, pp. 679–693, 2002.
- [37] D. A. Boas, J. P. Culver, J. J. Stott, and A. K. Dunn, “Three dimensional Monte Carlo code for photon migration through complex heterogeneous media including the adult human head,” *Opt. Express*, vol. 10, no. 3, pp. 159–170, Feb. 11 2002.

- [38] A. M. Siegel, J. P. Culver, J. B. Mandeville, and D. A. Boas, “Temporal comparison of functional brain imaging with diffuse optical tomography and fMRI during rat forepaw stimulation,” *Phys. Med. Biol.*, vol. 48, no. 10, pp. 1391–1403, May 21 2003.
- [39] A. Y. Bluestone, G. Abdoulaev, C. H. Schmitz, R. L. Barbour, and A. H. Hielscher, “Three-dimensional optical tomography of hemodynamics in the human head,” *Opt. Express*, vol. 9, no. 6, pp. 272–286, Sept. 10 2001.
- [40] “NIRx Medical Technologies, LLC.” <http://www.nirx.net/products/dynot.html>, 2004.
- [41] C. H. Schmitz, H. L. Graber, H. Luo, I. Arif, J. Hira, Y. Pei, A. Bluestone, S. Zhong, R. Andronica, I. Soller, N. Ramirez, S. S. Barbour, and R. L. Barbour, “Instrumentation and calibration protocol for imaging dynamic features in dense-scattering media by optical tomography,” *Appl. Opt.*, vol. 39, no. 34, pp. 6466–6486, December 1 2000.
- [42] R. Choe, A. Corlu, K. Lee, T. Durduran, S. Konecky, M. Grosicka-Koptyra, S. Arridge, B. Czerniecki, D. L. Fraker, A. DeMichele, B. Chance, M. Rosen, and A. Yodh, “Diffuse optical tomography of breast cancer during neoadjuvant chemotherapy: A case study with comparison to mri,” *Med. Phys.*, vol. 32, no. 4, pp. 1128–1139, April 2005.
- [43] X. Zhang, V. Toronov, and A. Webb, “Integrated measurement system for simultaneous functional magnetic resonance imaging and diffuse optical tomography in human brain mapping,” *Rev. Sci. Inst.*, vol. 77, p. 114301, 2006.
- [44] B. W. Pogue, M. Testorf, T. McBride, U. Østerberg, and K. Paulsen, “Instrumentation and design of a frequency-domain diffuse optical tomography imager for breast cancer detection,” *Opt. Express*, vol. 1, no. 13, pp. 391–403, Dec. 22 1997.
- [45] J. J. Stott, “Introduction to optical breast imaging.” Presentation at MGH, available at <http://www.nmr.mgh.harvard.edu/~jstott/>, 2002.
- [46] T. O. McBride, B. W. Pogue, S. Poplack, S. Soho, W. A. Wells, S. Jiang, U. L. Østerberg, and K. D. Paulsen, “Multispectral near-infrared tomography: a case study in compensating for water and lipid content in hemoglobin imaging of the breast,” *J. Biomed. Opt.*, vol. 7, no. 1, pp. 72–79, January 2002.
- [47] E. Graves, J. Ripoll, R. Weissleder, and V. Ntziachristos, “A submillimeter resolution fluorescence molecular imaging system for small animal imaging,” *Medical Physics*, vol. 30, no. 5, pp. 901–911, May 2003.
- [48] G. Zacharakis, J. Ripoll, R. Weissleder, and V. Ntziachristos, “Fluorescent protein tomography scanner for small animal imaging,” *IEEE Trans. on Medical Imaging*, vol. 24, no. 7, pp. 878–885, July 2005.
- [49] A. J. Chaudhari, F. Darvas, J. R. Bading, R. A. Moats, P. S. Conti, D. J. Smith, S. R. Cherry, and R. M. Leahy, “Hyperspectral and multispectral bioluminescence optical tomography for small animal imaging,” *Phys. Med. Biol.*, vol. 50, pp. 5421–5441, 2005.